Scientia Horticulturae 339 (2025) 113844

Contents lists available at ScienceDirect

Scientia Horticulturae

journal homepage: www.elsevier.com/locate/scihorti

Research Paper

Grapevine and cover crop spectral response to evaluate vineyard spatio-temporal variability

Pietro Catania, Massimo Vincenzo Ferro *, Santo Orlando, Mariangela Vallone

Department of Agricultural, Food and Forest Sciences (SAAF), University of Palermo, Building 4, 90128 Palermo, Italy

ARTICLE INFO

Keywords:
Cover crop
Soil penetration resistance
NDVI
UAV
Grapevine

ABSTRACT

The use of cover crops in vineyards is considered a management strategy that contributes to improving soil structure. Remote sensing techniques of cover crops provide information on spatial variability that can be useful in precision viticulture. This study aims to investigate soil-plant interactions using biometric data, spectral response and soil physico-chemical parameters measured across 2021–2022, with the scope of assessing spatio-temporal variations of cover crop and vineyard. These evaluations were conducted on an on-farm vineyard in a semi-arid Mediterranean environment. During the winter season (T1), the cover crop (*Vicia Faba*) growth was evaluated. Equally, during the summer season (T2), vineyard monitoring was carried out during the phenological stages of flowering (T2A) and grape ripening (T2B). Multispectral images acquired through unmanned aerial vehicle (UAV) were employed, and subsequently, the normalized difference vegetation index (NDVI) was calculated to obtain crops vigor maps. Through bivariate LISA cluster maps, cover crop vigor maps were compared with those of the vineyard, revealing the presence of significant positive spatial autocorrelation between the two crops. Indeed, in areas where the cover crop exhibited higher dry matter accumulation, grapevine high vigor growth was observed. The spatial association identified in surveys conducted in T1 and T2 was examined considering soil parameters. It emerged that in areas where both the cover crop and the vines exhibited high NDVI values, soil factors such as soil organic carbon (SOC) content and total nitrogen (TN) were higher. Conversely, in areas where both crops showed low NDVI values, they were associated with higher soil bulk density (BD). Moreover, in low vigor zones, higher soil penetration resistance (SPR) values were observed in both T1 and T2, contributing to limiting root elongation and thus reducing overall crop growth. Vegetative growth variability observed through vigor maps and soil physicochemical properties was evaluated through principal component analysis (PCA). Soil parameters considered within these components highlighted their influence on crop growth. This study emphasizes how soil factors directly influence the spatiotemporal variability of crops. Monitoring cover crops allows for early detection of spatial variability, supporting vine growers in choosing sustainable vineyard management techniques.

1. Introduction

The vineyard agroecosystem represents a complex agricultural environment, where interactions between vines, soil, climate, and farming practices play a crucial role in grape quality production. In this context, understanding the dynamics of the vineyard agroecosystem is essential for optimizing farming practices, promoting environmental sustainability, and ensuring high enological standards. The importance of environmental sustainability in the grapevine sector is increasingly recognized, as traditional farming practices can have negative impacts on soil, water, and biodiversity (Puig-Montserrat et al., 2017). Intensive management of vineyards may result in soil compaction, depletion of water resources, and erosion, compromising the functionality of the agroecosystem. Crop operations and soil management systems can influence the soil physical properties over time, particularly about soil bulk density (BD) and soil penetration resistance (SPR), which are

Abbreviations: DOY, Day of the year; UAV, Unmanned aerial vehicle; SPR, Soil penetration resistance; BD, Bulk density; SOC, Soil organic carbon; WFPS, Soil water filled pore space; SWC, Soil water content; TN, Total nitrogen; VI, Vegetation indices; DTM, Digital terrain model; NDVI, Normalized difference vegetation index; PL, Plant length; FW, Fresh weight; DW, Dry weight; SL, Shoot length; TLA, Total leaf area; Chl, Leaf Chlorophyll; NBI, Nitrogen balance index; BiLSA, Bivariate local indicators of spatial association; OBIA, Object-Based Image Analysis; NIR, Near infra-red.

* Correspondence author.
E-mail address: massimovincenzo.ferro@unipa.it (M.V. Ferro).

https://doi.org/10.1016/j.scienta.2024.113844
Received 18 May 2024; Received in revised form 10 November 2024; Accepted 23 November 2024
Available online 4 December 2024
0304-4238/© 2024 The Authors. Published by Elsevier B.V. This is an open access article under the CC BY license (http://creativecommons.org/licenses/by/4.0/).

significantly influenced by soil tillage practices (Catania et al., 2013; Ozpinar et al., 2018). If soil penetration resistance exceeds the value of 2.5 MPa, it hinders root growth in the soil, compromising their ability to reach water and essential nutrients for growth (Whalley et al., 2007). This threshold has commonly been accepted as a critical point beyond which these negative effects occur. However, some studies have proposed a higher threshold for agricultural soils, highlighting the complexity of evaluating SPR and the importance of carefully considering specific soil conditions and the traffic caused by agricultural machinery (Carrara et al., 2007; Håkansson and Lipiec, 2000; Hamza and Anderson, 2005). Among the factors regulating soil physical properties, soil porosity is a dynamic process influenced by various factors, including soil water content and bulk density (Bhandral et al., 2007). In cases of inadequate porosity, roots may effort to obtain oxygen, compromising their metabolism and nutrient absorption capacity. Furthermore, oxygen is crucial for the decomposition of organic matter by microorganisms (Czyż, 2004; McArtney and Ferree, 1999). High temperatures and arid conditions typical of the Mediterranean area can accelerate the decomposition processes of organic matter in the soil. The practice of conventional tillage such as chisel plough and rotary tillers can promote the decomposition of soil organic carbon (SOC)(Laudicina et al., 2012), resulting in an increase in soil penetration resistance (Catania et al., 2018). Other observed phenomena include the association between losses of soil organic carbon and increased sediment erosion. These interdependent phenomena can influence the overall vigor of the vineyard (Karn et al., 2024; Novara et al., 2018). In this context, the practice of cover cropping in vineyard inter-rows proves to be a promising strategy to enhance overall sustainability. It contributes to improving soil structure by promoting the formation of stable aggregates, increasing SOC storage, reducing bulk density (BD) (Wheaton et al., 2008), enhancing porosity and promoting infiltration, as well as mitigating soil erosion (Kaye and Quemada, 2017; Novara et al., 2019). Additionally, cover crops enhance water infiltration, increase water retention capacity, and promote nutrient balance (Haruna et al., 2020). Research has confirmed a strong correlation between soil aggregate stability, soil structure, and organic matter content (Celik et al., 2010; Hati et al., 2007; Haynes and Naidu, 1998). Soil stable aggregates help to balance the ratio between macropores and micropores, consequently reducing BD (Dexter, 2004; Guzmán et al., 2019). Cover crops, including legumes, are characterized by their ability to contribute to soil nitrogen accumulation. The phenomenon of nitrogen rhizodeposition by legume roots represents a potential pathway from which vines could benefit (Wichern et al., 2008). However, the main nitrogen source resulting from the practice of legume cover crops is due to the decomposition and mineralization of the organic residues of legumes at the end of the growing season (Fillery, 2001). The amount of nitrogen derived from cover crop depends on a complex interaction of factors, including legume species, duration of the growing season, and soil and climatic conditions (Guerra and Steenwerth, 2012). In the Mediterranean area, high soil temperatures and rainfall occurring after the burial of biomass provide favourable conditions for rapid residue decomposition (Shennan, 1992). Through the fixation and decomposition of legume residues, a substantial amount of nitrogen (N) is stored in the soil. However, it has been found that the amount of N from legumes that is actually absorbed by cover-cropped vine plants is 12–15 kg N/ha^{-1}(Ovalle et al., 2010). The grapevine N uptake model depends on soil availability and management techniques. This can give rise to noticeable effects on vigor, regulating parameters such as canopy efficiency and shoot growth rate (Guerra and Steenwerth, 2012). Nonetheless, vineyard management in semiarid environments is complex, and one of the main challenges being competition for water and nutrients between cover crops and the vines. As a result, grapegrowers tend to use cover crops in a temporary mode, especially with legume species positioned in the inter-rows and then buried at the beginning of spring (Novara et al., 2011). The variations observed in the soil can directly influence plant growth, potentially affecting their spectral signature. More vigorous plants tend to have greater biomass, larger leaf area, and a balanced chlorophyll content, which may result in a different spectral signature compared to less vigorous plants. Crop growth monitoring can be carried out using vegetation indices (VI), utilizing information collected from sensors measuring radiation reflected by plants across different bands of the electromagnetic spectrum. More vigorous plants generally exhibit higher reflectance across most spectral bands. Among the vegetation indices, the normalized difference vegetation index (NDVI) is commonly used to assess crop growth variability, considering reflectance in the red and near-infrared bands (Rouse et al., 1974). Several studies have investigated the advantages of using multispectral sensors compared to traditional methods for crop monitoring. Among these technologies, unmanned aerial vehicles (UAV) are increasingly utilized as they enable more frequent and detailed monitoring of crops, thanks to the high spatial resolution of the images (Sozzi et al., 2020). Recent studies have shown that vigor maps derived from UAV, focusing solely on vine vegetation, provide an accurate representation of vineyard variability (Ferro et al., 2023; Filippetti et al., 2013; Pádua et al., 2019). NDVI has been extensively studied and demonstrated to be closely associated with various vegetative and physiological parameters of the vineyard, often used as a key factor for spatial management decisions in vineyards (Campos et al., 2021; Caruso et al., 2017, 2023; Matese and Di Gennaro, 2021). Understanding vineyard variability is of strategic importance, as capturing the dynamics related to soil physical and chemical properties, as well as climatic factors, is essential for determining the sources of spatial variability (Gatti et al., 2022; Pereyra et al., 2023). Yuan et al. (2019) identified strong linear correlations between cover crop biomass and NDVI, demonstrating that UAVs are valid tools for obtaining relatively rapid and non-destructive estimates of biomass. Damian et al. (2017) evaluated the effect of variability caused by organic residues and released nutrients from cover crops on the yield of subsequent main crops, using estimates based on NDVI maps calculated from UAVs. Crop cover remote sensing can be used as a 'reflector' or 'bio-indicator' of soil conditions. Futerman et al. (2023), leveraging this concept, proposed the use of prescription maps for the primary crop's basic fertilization, relying on maps depicting the variability of cover crop vigor. The spatiotemporal assessment in precision agriculture is carried out by considering Local Indicators of Spatial Autocorrelation (LISA). These consist of specific indices to evaluate the presence of spatial clusters or simultaneous spatial dispersions for two variables in a specific area (Anselin and Rey, 2014). These statistical methods have recently been applied to images acquired from UAVs, aiming to compare different vegetation index maps of a vineyard with other maps related to parameters derived from in-situ ground characterizations (Matese et al., 2019; Pastonchi et al., 2020).

Based on these studies, site-specific variability corresponding to cover crop and vineyard across two different seasons of the crop cycle was investigated. A comparative study was conducted considering the main factors influencing plant growth, including soil physical and chemical properties, and crop biometric data that determine variations in their spectral response.

2. Materials and methods

2.1. Study area and experimental design

The experimental vineyard under study is in southern Italy, specifically in the Bianco Alcamo protected designation of origin (PDO) area (37°55′12 "N and 13°04′27 "E). Based on the methodology of an on-farm experiment, a study was conducted in 2021–2022 in a 16-year-old vineyard located in Camporeale (Palermo, Italy) at Tenuta Rapitalà (Fig. 1a). The trial was carried out in a drip-irrigated vineyard cultivar 'Cattarratto' vines grafted onto 140 Ru rootstock. Vineyard had a planting distance of 2.40 m between rows and the vines are spaced at a fixed distance of 1 m. Rows are North-East-South-West (NE-SW) oriented with a double cordon training system. The vines were pruned to

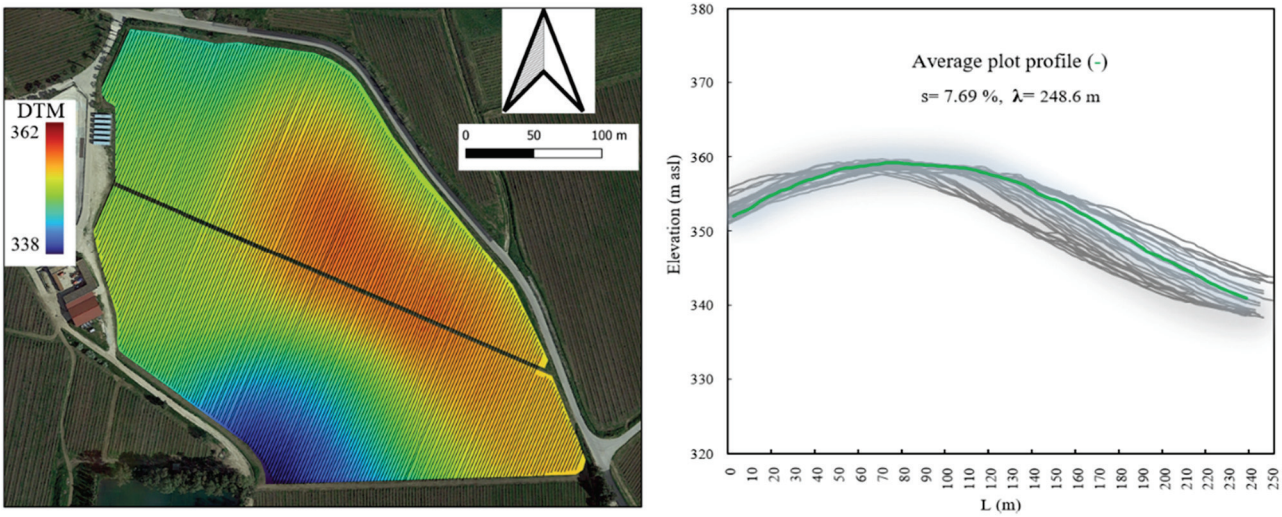

Fig. 1. a) Experimental site location, coordinates of field centroid: 37°55′11.18′′ N, 13°04′22.31′′E.
b) Graphical representation of the average slope of the vineyard rows.

two buds per spur, each spur being spaced approximately 0.15 m apart. The vertical canopies were managed with three sets of double wires for foliage and individual shoot positioning. The area is characterized by a Mediterranean climate (summer drought) according to Kottek et al. (2006). The climate of this area is classified as Csa and can alternatively be described as semi-arid according to the Thornthwaite moisture index (Peel et al., 2007). Rainfall is distributed throughout autumn, winter, and spring, with the highest rainfall intensities observed during the autumn season. Mean air temperature ranging from 18.3 to 24.6 °C, while mean annual rainfall from 700 to 820 mm. The total experimental area is 8 hectares with irregular orography and elevation ranging from 340 to 369 m above sea level. The graph in Fig. 1 shows the average planar slope of the plot under investigation. Considering plot average length "λ" (m) and digital elevation model (DEM) values (Fig. 1b), it was possible to determine the average slope, which is 7.69 %.

The soils are vertisols with typical characteristics of clayey soils according to FAO (2006). The main soil properties, determined before setting up the experimentation and referring to 0–0.20 m soil layer are reported in Table 1. Soil texture, reaction (pH) and electrical conductivity (EC) were determined in the laboratory. Soil reaction was measured in distilled water using a soil/solution ratio of 1:2.5 (w v-1) and a glass membrane electrode, while soil EC was determined in distilled water using a soil/distilled water ratio of 1:5 (w v-1). The soil is characterized by a clay loam texture with pH equal to 7.66 and 0.19 dS m^{-1} cation exchange capacity.

Before cover crop sowing in October 2021, tillage was carried out with a horizontal spring tiller with 7 chisel-type shares, at a depth of 0.15 m. Subsequently, a legume species (*Vicia fava* L.) was sown as cover crop. This cover crop was seeded using a combined power harrow with a mechanical seed drill, in the beginning of November 2021. Sowing was carried out in vineyard in the inter-row areas, 0.20 m row spacing, and 0.05 m depth, with the amount of 90 kg ha^{-1}. Cover crops were mechanically buried by plowing in the 0.20 m depth in spring (mid-April). After the cover crop was buried and topsoil aerated, the vineyard was managed following the traditional agronomic practices applied in semi-arid climate zones. The soil was managed according to standard agronomic practices, three shallow tillages (0.15 m depth) were carried out from spring to summer to control weeds, prevent crust formation and, finally, reduce soil evaporation.

Table 1
Basic properties of soil sampled and measured before the experiment in March 2021.

Soil properties	Value
Sand (0.02 < Φ < 2 mm, g kg^{-1})	388 ± 12
Silt (0.002 < Φ < 0.02 mm, g kg^{-1})	226 ± 14
Clay (Φ < 0.002 mm, g kg^{-1})	378 ± 15
pH in water	7.66 ± 0.1
Electrical conductivity (dS m^{-1})	0.19 ± 0.03

2.2. Data survey

To assess crops spatial and temporal variability, ground and remote surveys were performed (Fig. 2). Ground surveys were carried out to measure agronomic parameters and vegetative crop growth, while remote surveys were carried out using a UAV, evaluating plant spectral response. Temporal variability was assessed across three distinct periods, each corresponding to specific days of the year (DOY). The first survey period was conducted at DOY 63, during winter, when the vineyard was dormant. At this time, the spatial variability of cover crops was evaluated through vegetative measurements and spectral surveys, with cover crops in the full flowering stage. The second survey period occurred at DOY 169, during the vineyard's growing season, with assessments of vegetative and spectral characteristics of the vine at the phenological stage of fruit set (BBCH 65). The third survey period, at DOY 226, also during the growing season, involved similar measurements, with the vine at the grape ripening stage (BBCH 85).

2.3. Agronomic sampling

The sampling points were identified in areas with different vigor, excluding the most external part of the field. The identification of zones with different vigor levels was conducted through an integrated analysis of agronomic parameters and vegetation maps derived from multispectral data. Vineyard vegetative growth from the bud break stage were assessed by measuring shoot length (m) and number of leaves per shoot. Similarly, in situ agronomic surveys were conducted on cover crops to assess the evolution of plant length (m). On-site agronomic trait variations measured in were compared with vegetation vigor maps. This analysis made it possible to identify field zones with different vegetative growth levels. A total number of 20 experimental units were selected from both the vineyard and cover crop at the same location (Fig. 3). In

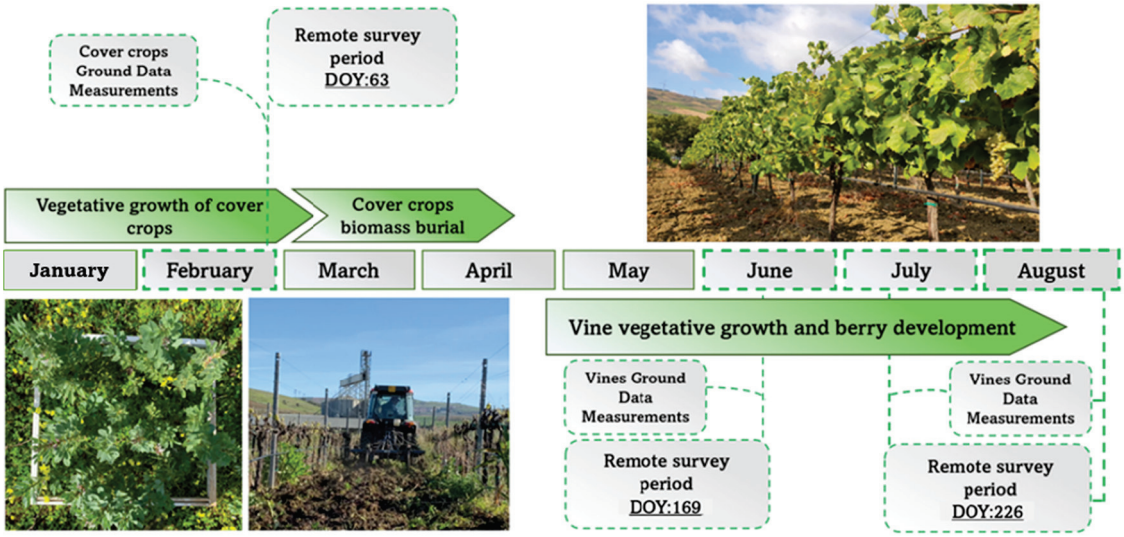

Fig. 2. Flow chart of the biometric and multispectral surveys carried out on cover crop and vineyard.

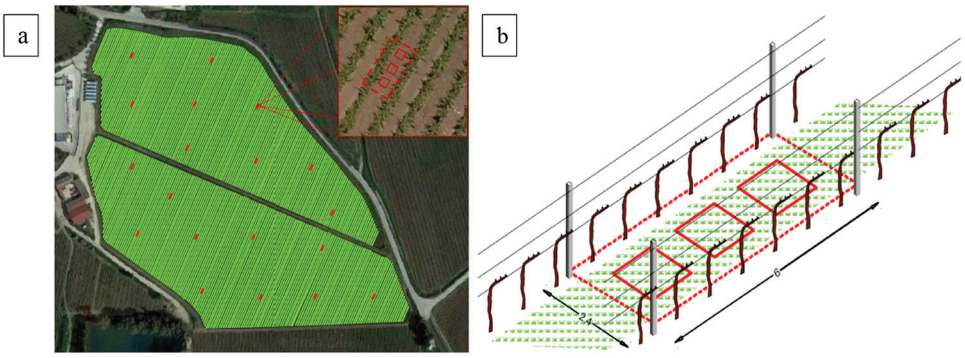

Fig. 3. a) Representation of the experimental units in the field and configuration of the three sub-samples. b) Graphic representation of an experimental unit where the vineyard sampling zones are highlighted in red with dashed lines, and for the cover crops with squares.

the case of the vineyard, the experimental unit corresponds to a row section with a length of 7 m that includes 6 vines. For cover crop, each experimental unit was divided into three subsamples ($n = 3$ replicates for each sample block).

Each sub-sample used to evaluate cover crop biometric parameters was identified using a 1 m^2 square, placed in the central part of the inter-row, alongside each experimental unit of vineyard. In the aboveground cover crop sub-sampling area, three agronomic parameters were evaluated: plant length (PL) m, fresh weight (FW) g and dry weight (DW) g. Fresh weight was measured using a digital balance (Shimadzu ATY324R, Milan, Italy). Plant material was clipped at soil level and weed and cover crop biomass was separated. These samples were dried at 60 °C for 48 h until a constant weight was reached to determine their dry weight.

Surveys on the vegetative parameters were carried out in the vineyard selecting the same 20 experimental units used in the cover crop sampling. Each experimental unit consisted of six vines anda total of 120 vines were monitored. In Fig. 3b, the sampling blocks are shown for both the cover crops and the vineyard. The dashed red line refers to the vineyard sampling area. Conversely, the squares marked with a solid red line denote the sampling points for the cover crops. The vegetative parameters were shoot length (SL), leaf counts for each shoot (LS), total leaf area (TLA), epidermal chlorophyll (Chl) and nitrogen balance index (NBI). The TLA of primary and lateral shoots was measured using an LI-3100C area meter (Li-COR Environmental, 4647 Superior Street Lincoln, NE, USA). Chl and NBI values were measured with the Dualex 4 leaf-clip version (Dualex Scientific+, Force-A, Orasy, France) on fully expanded leaves at the second phenological stage of sampling. Chlorophyll $a + b$ was estimated from near-infrared (NIR) transmittance measurements at 710 and 850 nm, it was used as data from the device without transformation. NBI serves as an indicator of the nitrogen status within the vines and is calculated by considering the ratio of chlorophyll to flavonoid content (Tremblay et al., 2012). The average value of Chl and NBI were calculated at two separate points on the epidermal surface for each leaf.

2.4. Determination of soil physical and chemical properties

Soil samples were collected during two time intervals, in autumn (DOY 338), which corresponds to the rainy season in the southern Mediterranean region, and in summer (DOY 217). Sampling was conducted during both 2021 and 2022 to ensure comprehensive data collection across different climatic conditions. Soil rings of 98 cm^3 for the first 0.20 m layer were used to determine bulk density. The soil bulk density (BD) was measured following the protocol of Blake and Hartge (1986), using intact samples collected with a steel rings with 0.05 m diameter and height. Gravimetric soil water content (SWC) was determined by weight difference between fresh and dried (24 h at 105 °C) sample. Soil water filled pore space (WFPS) was calculated considering the SWC, BD, and taking into consideration the soil absolute density (AD) equal to (2.65 g cm^{-3}). The calculation follows the analytical formula [1] presented below:

$$WFPS = \frac{SWC * BD * 100}{(1 - BD/AD)} \quad (1)$$

At these sampling points, soil penetration resistance (SPR) measurements were conducted. SPR was assessed down to a depth of 0.60 m using a portable digital penetrometer (Eijkelkamp Penetrologger mod. 06.15, Netherlands, Giesbeek), equipped with a load cell, an ultrasonic depth sensor, a data logger, and a probing rod. It culminates with a cone having a base area of 200 mm^2 (compliant with ASAE standard 313.1) (ASAE, 2009). Capable of measuring penetration force from 0 to 1000 N with a resolution of 1 N, it can assess soil resistance up to a depth of 0.80 m with a resolution of 10 mm (Carrara et al., 2007). Two measurements per second were recorded. Soil chemical analyses were carried out on samples which were air-dried and sieved at 2 mm. Soil organic carbon (SOC) and total nitrogen (TN) were determined on pulverized soil samples by dichromate digestion (Nelson and Sommers, 1983) and for total N by the Kjeldahl method. Cation exchange capacity (CEC) was determined with ammonium acetate solution buffered at pH 7.0 (Sumner and Miller, 1996).

2.5. UAV configuration and data acquisition

A remote UAV platform equipped with a multispectral and RGB camera was used to investigate the spectral features of cover crop and vine. The DJI model Phantom 4 (DJI, Shenzhen, China) is a quadcopter with four rotating wings and vertical takeoff and landing (VTOL), described in detail in (Ferro and Catania, 2023). The multispectral camera consists of five independent sensors 1/2.9″ CMOS, operating in the blue band at 450 nm, the green band at 560 nm, the red band at 650 nm, the red edge at 730 nm, and the NIR band at 840 nm. All the sensors have a spectral sensitivity range of ±16 nm around their nominal wavelengths, except for NIR sensor, which has a wider spectral sensitivity range of ±26 nm. The camera is equipped with a sixth sensor capturing images in the visible spectrum.

The UAV flights were conducted in three dates throughout the cover crop and grapevine growth cycle (Table 2). The first flight was conducted during the winter season in February (T1) to assess cover crop spectral response (DOY 63). Subsequently, two surveys were performed in vineyard corresponding to the late flowering stage (T2A) and at the grape ripening stage (T2B). All surveys presented the same setting characteristics.

Images were taken between 11:30 and 13:00 under clear skies, with no clouds, sunny conditions, and moderate wind. The automatic guide followed the predetermined set route and waypoints. The flight height was 70 m above ground level (AGL) using Real Time Kinematic (RTK) differential corrections, obtaining a ground sample surface (GSD) of 0 .037m. The image acquisition was performed at an average speed of 6.9 ms^{-1} in stop-and-go mode. The front and side overlap percentage between the image was 70 %, while the gimbal pitch was set at 90° (downwards). Prior to and following each flight, images were acquired using specific reflectance calibration panels. Image acquisitions in TIFF format were performed to carry out radiometric calibration in post-processing. To enhance the accuracy of survey, 20 Ground Control Points (GCPs) were positioned both externally and internally within the field. GCPs were georeferenced using the GNSS receiver S7-G by Stonex (Italy, Milano), equipped with a Stonex geodetic antenna in RTK mode as an average of 60 measurements. The GCPs were imported into the QGIS software, version 3.28 (QGIS Development Team, 2021), and all orthomosaics were geometrically corrected.

Table 2
Sampling date and corresponding phenological growth stages.

Survey	Description	BBCH code
T1	Cover crop flowering	–
T2A	Grapevine flowering stage	65
T2B	Grape ripening stage	85

2.6. UAV image processing and analysis

Georeferenced multispectral images were mosaicked using Agisoft Metashape Professional Edition version 1.7.3 software. The total number of images obtained for each individual survey and sensor was 215. All multiband images were uploaded into the software, followed by image alignment, GCP (Ground Control Points) loading, and reflectance calibration. Utilizing calibration panel images, reflectance was corrected using Agisoft Metashape software**.** Subsequently, the images containing the calibration panel were selected. Then, leveraging the reflectance calibration function within software, the correct reflectance values were determined. Finally, the dense cloud and the orthomosaic multiband were constructed for each survey (Hirschmuller, 2005). NDVI map was calculated using the near infra-red (NIR) and Red reflectance band maps, according to Rouse et al. (1974) equation, using QGIS software (Bollas et al., 2021). This vegetation index (VI) was calculated to investigate the spectral canopy conditions and identify the vigor level. For the high-resolution images acquired by UAV, it was necessary to perform a segmentation process of the NDVI images to differentiate the vineyard canopy rows from soil and shaded pixels, which classifies the input pixels into several different classes. Vine canopy segmentation and classification process was performed using the Object-Based Image Analysis (OBIA) method. For image segmentation, the Orfeo Toolbox library was employed, leveraging the large-scale mean-shift (LSMS) algorithm developed by Michel et al. (2014). Subsequently, the object image classification was performed using the supervised classifier namely support vector machines (SVM).

Remote sensing was useful for identifying sampling points and providing spatial input for the model, as previously ascertained by other authors (Basso et al., 2001). In the vineyard, SL, LS, and TLA were used to characterize three different zones of vine vigor, namely low vigor (LV), medium vigor (MV), and high vigor (HV). These assessments were carried out at both the T2A and T2B phenological stages. Vigor variability assessment was also conducted for cover crop, in situ agronomic assessments were performed during winter, and zones with different vegetative growth levels were identified. Cover crop vigor levels were characterised by evaluating the agronomic parameters PL (m) and FW (g). By assessing these agronomic parameters and comparing them with the variability detected through NDVI maps, three distinct vigor zones were identified, HV, MV and LV respectively. The three clusters of each map were identified using the K-means algorithm through the utilization of the SAGA library in QGIS.

The ordinary kriging interpolation method was used to create continuous vigor maps for cover crop and vineyard. Kriging interpolation implies that the estimation of an arbitrary point in a defined zone of the field is expressed with a linear weighting of all the observations. In order to provide the best linear estimate, semivariograms considering the spatial structure were calculated as made in previous studies (Chiles and Delfiner, 2009; Webster and Oliver, 2007).

The spatial structure of each vigor attribute of both crops was characterized and quantified using the experimental semivariogram, which was adapted using linear, linear with sill, spherical, exponential, and Gaussian theoretical models. The graph of the experimental semivariogram was obtained by calculating the semivariances at different distance intervals. For each model, we determined the following parameters: nugget variance (C_0), contribution (C1), sill variance (C_0+ C1) and range (a). The selection of the theoretical semivariogram model that was most suitable to represent the vigor variability in different phenological stages for both crops, was made according to the highest coefficient of determination (R^2).

2.7. Statistical analysis

The dataset, which includes sampling measurements of soil

parameters, cover crops and vineyard properties, as well as biometric data from UAV-based multispectral surveys reflecting vegetation spectral response, was subjected to statistical analysis. Primarily, descriptive statistics including mean, maximum, minimum and standard deviation values were calculated for the entire dataset. Afterwards, a multivariate statistical analysis was performed, with analysis of variance (ANOVA). The significance level (α) was set at 99 % ($p < 0.01$). The null hypothesis (H_0) for comparison between groups indicates that all means are equal, while the alternative hypothesis (H_1) is that not all means are equal. Tukey's multiple comparison test was used to identify the different means.

In this study, the bivariate local indicators of spatial association (BiLISA) was calculated, which is a measure of spatial autocorrelation assessing the association between two different variables, unlike the Moran's I (MI) which evaluates the autocorrelation of a single variable. To evaluate the global spatial autocorrelation of the data in an specific area, the statistical index I developed by (Moran, 1948) was measured according to equation [2] (Legendre and Fortin, 1989):

$$I = \frac{n}{W} * \left[\frac{\sum_{i=1}^{n} \sum_{j=1}^{n} w_{ij}(x_i - \bar{x}) * \left(y_j - \bar{y}\right)}{\sum_{i=1}^{n} \sum_{j=1}^{n} w_{ij}} \right] \quad (2)$$

where n represents the number of observations, in our case 817, corresponding to the number of points derived from the regular grid used for each map; x_i, y_j represent the observed values of the two variables located at points i, j; $\bar{x}, \bar{y}$ are the average of the two variables of the n observed points of the NDVI attribute. In this equation, the spatial weights matrix (w_{ij}) with value 0 in the diagonal ($w_{ii}=0$) is considered; the sum of all spatial weights w_{ij} is represented by the spatial weight matrix W. The Python library PySAL was employed to calculate distance-based weights among observation points (Rey and Anselin, 2009). Process starts by establishing a matrix of spatial weights, whereby the coordinates of the sampling points are defined in a two-dimensional array (x, y). A threshold value of 5 was established, indicating the maximum distance within which points are considered adjacent, beyond this threshold, the weights are set to zero. Finally, a Gaussian kernel function was applied to modulate the intensity of the weights based on distance. MI index was calculated to evaluate the spatial autocorrelation in adjacent area. The MI index ranges from −1 to +1, where positive spatial autocorrelation implies similar values in neighboring locations, while negative spatial autocorrelation indicates dissimilar values in neighboring locations. A null value (MI = 0) suggests that there is no spatial autocorrelation, and that the spatial arrangement is completely random. The result is a pseudo p-value for each location, which can be used to assess significance.

The calculations to assess the local spatial dependence of NDVI related to cover crop and vineyard were performed using the GeoDa software, which provides the capability to manage spatial weights.

Computations for processing descriptive statistics and performing multivariate analysis ANOVA were performed using R software (R Core Team, 2023) and Microsoft Excel. Principal Component Analysis (PCA) was conducted to assess the relationship between NDVI values of cover crop and vineyard, along with other variables. This analysis was performed using *prcomp()* function in R, which facilitates the grouping of NDVI data, as well as agronomic parameters from soil, cover crop, and vineyard, into statistical factors. PCA aims to create linear independent variables that eliminate multicollinearity and effectively summarize the space-time information collected. PCA results were visualised to highlight trends, and they were saved for further examination of potential correlations among crop vigor zones.

3. Results

3.1. Assessment of cover crop and vineyard variability

In this section, the findings of the analysis exploring temporal variability between period T1 and T2 are presented. This investigation proposes a visual comparison of temporal variability evolution, providing an in-depth insight into the growth dynamics over time of both the cover crop and the vineyard. Through a detailed analysis of data collected at different times, the aim is to identify any trends,

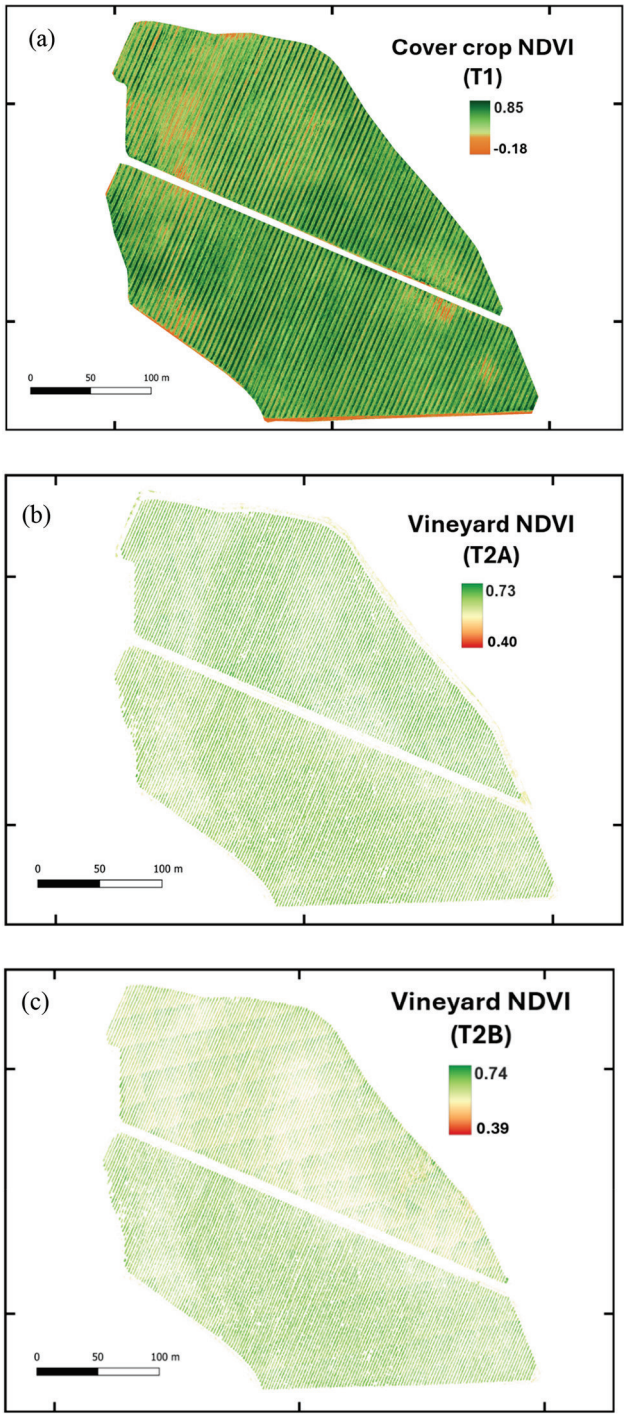

Fig. 4. Representation of NDVI for cover crop (a) and vineyard canopy variability detected by UAV during T2A (b) and T2B (c).

variations, or distinctive patterns in crop growth.

In Fig. 4a, the NDVI map representing cover crop spectral response is depicted. This survey was conducted during T1 phase, when cover crop was at flowering stage, characterized by the highest biomass accumulation and, consequently, the most significant period of vegetative activity. Fig. 4b and 4c, on the other hand, illustrate the results of vine canopy NDVI. Table 3 presents the results of descriptive statistics for the NDVI evaluated during the three investigation periods, referring to the conditions of the cover crop during the winter period (T1) and to the vineyard during the summer period (T2A and T2B). These results aid in understanding the vigor maps through an analytical approach. Referring to period T1, it is observed in Table 3 that the most represented area is HV, covering an area of 48,900 m^2, followed by low vigor areas for the cover crop (18,700 m^2). The area with moderate vigor is slightly lower, totalling 14,200 m^2. The average NDVI value associated with these areas is well differentiated across the three vigor levels. It is noted that high vigor is represented by an average value of 0.74±0.083, differing from the one of medium vigor, which is 0.59±0.074. Conversely, the low vigor of the cover crop shows an NDVI value of 0.32, considerably lower than that observed for the other levels. In this case, very low NDVI (−0.18) with a high standard deviation were observed. This result could be caused by the cover crop humidity observed during the survey that could significantly influence the spectral response, as water can attenuate a greater amount of radiation in the near-infrared (NIR) band. The effect could be a decrease in NDVI, as the index is based on the difference between reflectance in the red band and that in the near-infrared band. For the other two vigor levels, the observed minimum value is approximately 0.2, with maximum NDVI values reaching around 0.8. Table 3 displays the results related to the vineyard, showing that during T2A period, the largest area exhibits medium-high vigor. This is reflected by an NDVI range from 0.66 ± 0.043 to 0.72 ± 0.046. A similar trend is observed in period T2B, where HV areas constitute approximately 50 % of the plot, while areas with medium and low vigor account for 25 %. However, it should be noted that LV areas underwent an increase of 11 % between period T2A and T2B. Conversely, the MV area decreased by 11 % over the same period. The areas identified as high vigor remained stable between the two phenological periods considered. Concerning NDVI observed during vineyard growth cycle, it can be stated that they differ from those observed for cover crop. Indeed, both for the periods T2A and T2B, the range of variation among the three vigor levels is smaller compared to cover crop NDVI. Particularly, during T2A survey, average values of 0.72 for HV, 0.65 for MV, and 0.60 for LV were observed. This trend of NDVI values remains relatively stable throughout the vineyard growth season, as also observed for period T2B. In fact, the average NDVI value decreased by 6 % from June to August, 5 % in the case of MV, and 9 % in the case of LV. In general terms, LV reported a higher standard deviation value in both investigation periods.

The maps in Fig. 5 illustrate vigor spatial distribution in three distinct classes during the monitoring phases of cover crop T1 and vineyard T2. The vigor maps were generated using kriging interpolation to differentiate growth levels. Green indicates areas of high vigor and reflects high growth, light green represents areas of medium vigor and is associated with medium growth, white identifies regions of low vigor and indicates low crop growth.

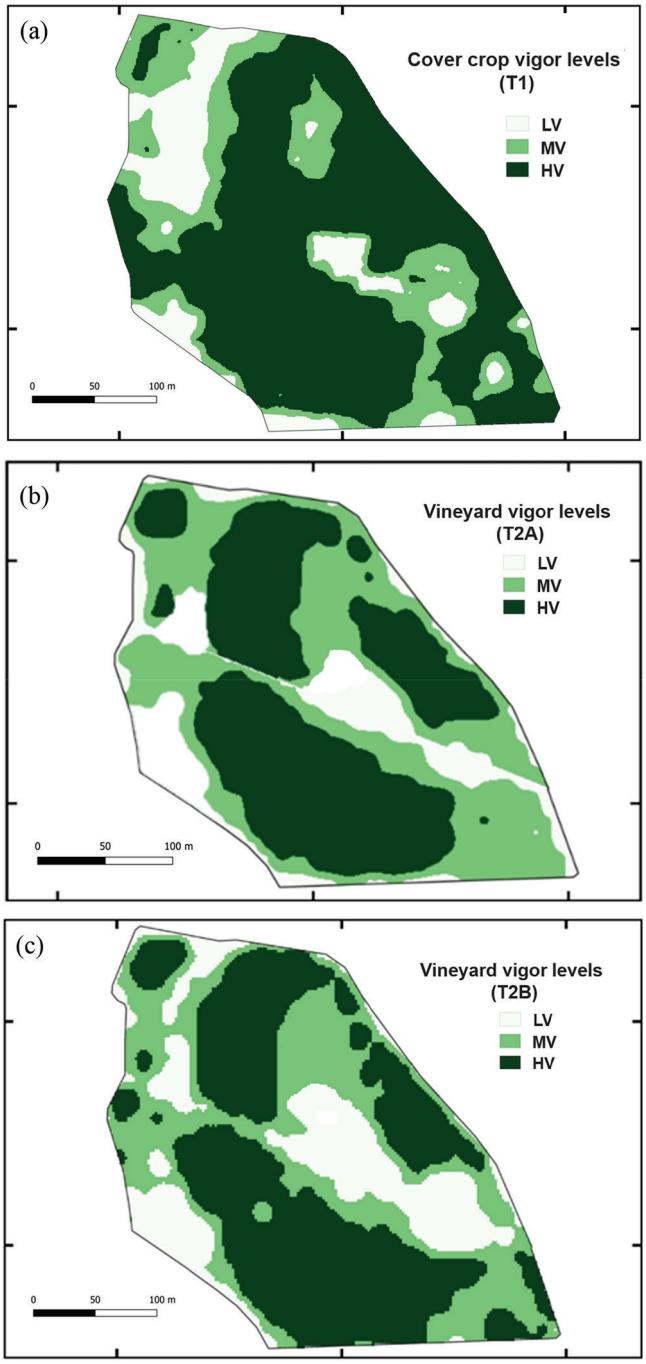

Fig. 5. Vigor maps obtained by application of kriging interpolation. Figure (a) show cover crop vigor map and vineyard vigor map for two surveys T2A (b) and T2B (c).

Table 3
Summary statistics of NDVI and the distribution of extension vigor areas results for cover crop (T1) and vineyards in the two survey phases (T2A and T2B).

	Vigor levels	Extension area (m^2)	Mean	Min	Max	Standard deviation
T1	HV	48.900	0.745	0.233	0.814	0.083
	MV	14.200	0.590	0.211	0.734	0.074
	LV	18.700	0.323	−0.183	0.654	0.097
T2A	HV	40.300	0.725	0.505	0.763	0.046
	MV	30.700	0.663	0.465	0.735	0.043
	LV	10.800	0.602	0.419	0.722	0.056
T2B	HV	40.500	0.682	0.662	0.738	0.014
	MV	21.200	0.630	0.618	0.664	0.012
	LV	20.100	0.549	0.381	0.619	0.047

The vegetative parameters of the cover crop were investigated. The analysis of variance ($p = 0.01$) clarified a certain significance of the observed differences in terms of cover crop development between the vigor zones. Table 4 shows that plants grown in an area classified as HV had an overall length by 40 % greater than plants grown in LV zone. A similar reasoning applies to the comparison between the length of MV plants and those from LV zones; the latter showed an overall reduction in development of 37 %. These differences in cover crop development impact their biomass accumulation. Indeed, plants with a greater overall

Table 4
Vegetative parameters assessed during period T1 and T2 periods are represented with means ± *S*.E. Different letters indicate statistically significant differences between vigor levels (p-Value < 0.01).

Crops parameters	Vigor level		
	HV	MV	LV
T1			
Plant Length (m)	0.82 ± 0.10 **a**	0.80 ± 0.13 **a**	0.58 ± 0.06 **b**
Fresh weight (kg)	1.53 ± 0.45 **a**	1.64 ± 0.35 **a**	0.95 ± 0.01 **b**
Dry weight (kg)	0.33 ± 0.06 **ab**	0.38 ± 0.01 **a**	0.25 ± 0.02 **b**
T2			
SL (m)	1.09 ± 0.23 **a**	0.92 ± 0.30 **ab**	0.68 ± 0.21 **b**
LS (n)	15 ± 3.0	12 ± 1.7	10 ± 3.2 **n.s**
Bunch/vine (n)	13 ± 2.2	10 ± 1.8	8 ± 1.9 **n.s**
TLA(m^2)	2.78 ± 0.36 **a**	2.48 ± 0.49 **a**	1.91 ± 0.18 **b**
Yield/vine (kg)	2.31 ± 0.37 **a**	2.39 ± 0.10 **a**	1.47 ± 0.24 **b**

length accumulate more biomass. In fact, plants from MV zones report a higher fresh weight by 70 % compared to LV plants. Tukey's test confirms that both for plant length and fresh weight, the HV and MV groups are not statistically different; instead, statistically significant differences are reported for both groups when compared to LV plants. Cover crop dry weight was also considered; it allows to evaluate the quantity of organic matter or biomass produced. Dry weight provides a more accurate estimate of the total plant biomass, as it considers only the organic matter present in plant tissues, not including water. In line with these observations, regarding dry weight, plants from MV zones exhibit the highest growth compared to the other two vigor levels. Specifically, the latter display a weight greater by 50 % compared to LV plants, a difference confirmed by the Tukey test. The group of plants cultivated in HV areas, on the other hand, is intermediate between the MV and LV vigor groups. Nevertheless, even plants grown in these areas show a 32 % dry weight increase compared to LV plants, which record the lowest weight. The results of the biometric analysis and vineyard yield, conducted during the summer growth season, are presented in Table 3. Regarding vegetative growth, it was observed that in terms of overall SL, vines developed in areas characterized by HV exhibited approximately 60 % higher growth compared to vines grown in LV zones. Consistent with this result, the analysis of TLA per plant provided clear findings regarding the overall canopy growth of the vineyard. Indeed, vines from HV and MV zones collectively showed a statistically significant 40 % greater TLA value compared to LV. The growth trend of vines developed in different vigor zones is also reflected in terms of production, as yield per plant measured at harvest. Higher yield was identified in vines displaying greater vegetative growth; actually, vines from HV and MV zones showed a 60 % increase of yield per plant compared to LV vines.

During the growth season, data on chlorophyll (Chl) content in leaves were evaluated. The results presented in Fig. 6a were obtained during the berry set stage, corresponding to the month of June (T2A). The Chl content per leaf unit (μg cm^{-2}) assessed for the three vigor levels further characterizes the vineyard. In HV and MV zones, there is a 15 % higher Chl content compared to LV areas. This trend is primarily observed during T2A. However, during T2B, MV and LV vineyard areas show an overall decrease in Chl content, corresponding to 25 % and 19 %, respectively. These differences between the two periods are confirmed by the Tukey test. Conversely, vines in HV zones did not exhibit a statistically significant decrease. The Chl content during T2B shows statistically significant differences between HV and LV vines, with HV vines showing a 34 % higher Chl content compared to LV. In addition to leaf Chl content, nitrogen status was also monitored. The analysis of variance on nitrogen balance index (NBI) revealed differences between low and high NBI values. HV was statistically different from LV ($p < 0.01$), with an NBI value 24 % higher. However, regarding the phenological phase of grape ripening, the highest value was observed for the MV vines. The comparison between the two phenological periods, T2A and T2B, showed an overall 45 % reduction in vineyard nitrogen status from the berry set phase to berry ripening.

3.2. Spatial-cluster analyses

The scatter plots in Fig. 7 illustrate the results of the global Moran's statistics and the bivariate analysis of spatial correlation between two geographically associated variables. The plot shows four areas that describe the spatial relationships between the variables, with positive clusters of high values in the upper right and low values in the lower left, while the opposite quadrants indicate negative relationships. The "non-significant" points indicate the absence of spatial correlation. The results presented in the scatter plot in Fig. 7a show a significant spatial autocorrelation ($p < 0.05$) between map T1 and map T2A with a Moran I value of 0.48. The positive correlation between the vigor index of period T1 and period T2B is even stronger, with a Moran I value equal to 0.54. This indicates that the spatial variability identified in the winter season, related to the cover crop, corresponds to the variability identified in the vineyard. However, the results indicate that soil and its physicochemical characteristics play a crucial role in both periods of investigation. The analysis of spatial correlation is confirmed by observing the Moran I value referred to the phenological stages T2A and T2B (Fig. 7c), obtaining a value of 0.73, indicating a close correspondence of the vineyard vigor macro-areas throughout the growing season.

The patterns in Fig. 8 indicate the spatial association between cover crop vigor (T1) and vineyard vigor (T2B). This map of spatial association between the two times has been provided to demonstrate the correspondence between homogeneous management zones. Four different colors are used in this map to represent four different types of local spatial autocorrelation. The green color denotes points where a high-high correspondence between the two variables was observed.

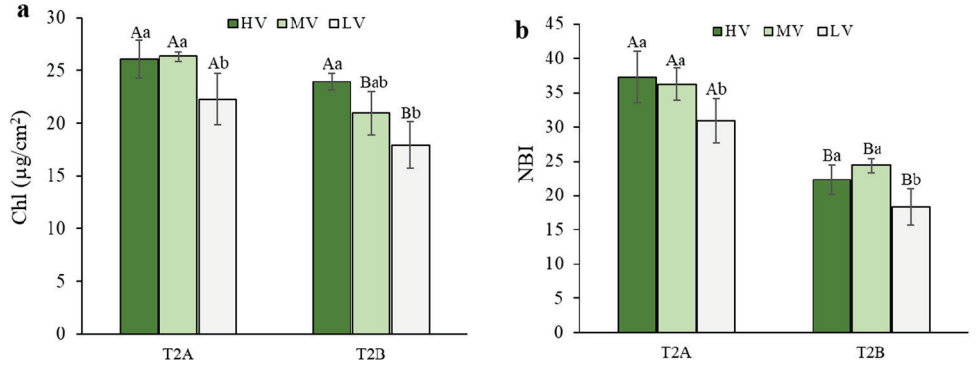

Fig. 6. Evaluation of leaf chlorophyll content (Chl) (**a**) and NBI (**b**) for the three-vineyard vigor in two phenological periods. Data were subjected to two-way ANOVA (Tukey's test, p-value <0.01) capital letters indicate statistically significant difference between the two periods, while the lowercase letters indicate differences between the vigor levels. ± SE is shown with the bars.

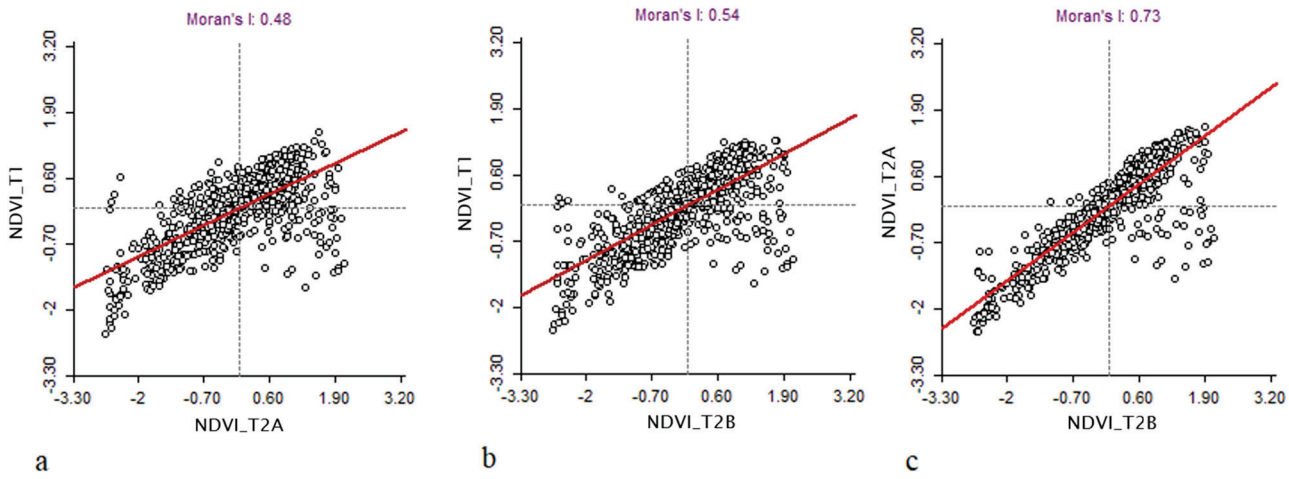

Fig. 7. Moran scatter plots to assess the local spatial autocorrelation of vigor maps for the three periods. a) comparison between T1 and T2A; b) comparison between T1 and T2B; c) comparison between T2A and T2B.

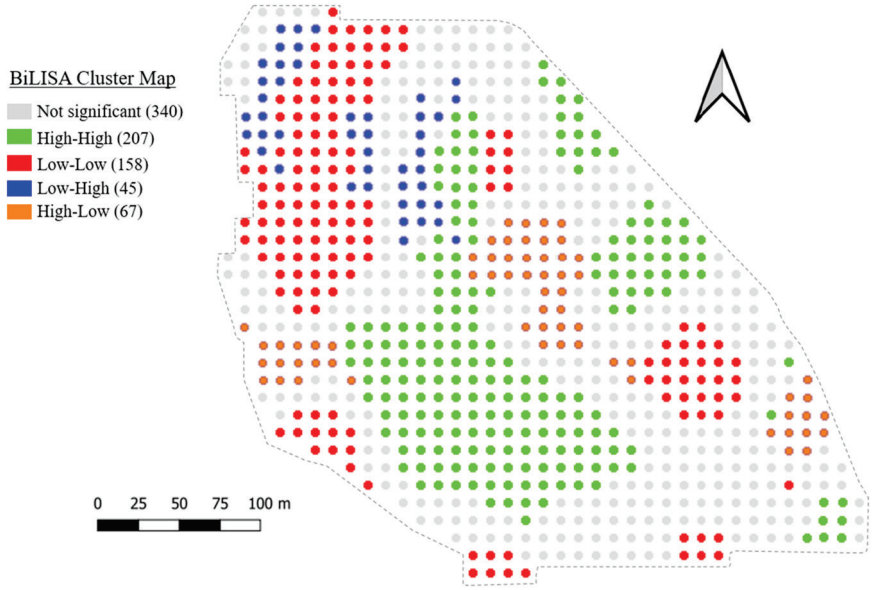

Fig. 8. BiLISA cluster maps between cover crop NDVI (T1) and vineyard NDVI (T2B).

Conversely, the red color indicates a low-low spatial autocorrelation between the variables. The blue and orange colors indicate points where a negative correlation between the variables was observed. The blue color represents points where the T2B map shows high vigor values, while the T1 map shows opposite values. Conversely, the orange points indicate zones where high vigor values were observed in the T1 survey, while the vineyard showed low vigor values at T2B. It is observed that points identified as high-high correspond to approximately 25 %, and points with a positive low-low autocorrelation account for 20 % of the total. Points with negative correlation represent a smaller percentage; for instance, low-high points account for 6 %, and high-low points for about 8 %. Meanwhile, points with gray coloring indicate areas with spatial correlations that do not reach significance ($p > 0.05$). Therefore, it was not possible to categorize them into any of the four observed cases, and at this level of significance, they exhibit a random spatial pattern. The comparison between seasons allows observing a relatively high stability of two clear large NDVI cluster patterns, showing a low-low association in the north-western part of the field and a high-high association in the central and south-western area of the field (Fig. 8). On the other hand, low-high points were mainly located near the low-low cluster area, whereas the high-low cluster distributes centrally and in the southwestern part of the field, adjacent to the High-High clusters. Therefore, cover crop NDVI is indeed associated with vineyard NDVI.

3.3. Evaluation of soil characteristics

The analysis of variance performed for the soil chemical-physical parameters (Table 5) displays both the F-test statistic values and the level of statistical significance. From the analysis of variance, F-test values were obtained, allowing the interpretation of which factors contributed most to increasing variability. Conversely, a high F-value indicates a case where the variability of group means is large compared to the variability within the group. In relation to the "time" factor, the null hypothesis, which assumes that the group means are equal, was rejected for the variables SWC, SBD, WFPS, and N, based on high F-values and particularly on the value $P < 0.01$. Regarding the "vigor level" factor, however, the null hypothesis was rejected for the variables SWC, SBD, SOC, and WFPS, except for the soil N content parameter. Regarding the interaction "time*vigor level", it was significant only for the variable

Table 5
Two-way ANOVA was conducted in the specific agroecosystem studied for the parameters soil water content (SWC), soil bulk density (SBD), soil organic carbon (SOC), water content and water-filled pore space (WFPS), and nitrogen content (N) (F-Value and p-value < 0.01).

Source of variation	SWC		SBD		SOC		WFPS		N	
	F-Value	P-Value	F-Value	P-Value	F-Value	P-Value	F-Value	P-Value	F-Value	P-Value
Time	846.43	<0.001	32.09	<0.001	0.18	0.681	733.91	<0.001	6.86	0.017
Vigor level	8.74	0.003	7.95	0.005	5.46	0.019	154.79	<0.001	0.99	0.396
Time*vigor level	2.16	0.152	10.97	0.001	0.04	0.961	201.36	<0.001	0.55	0.587

SBD and WFPS.

Regarding soil bulk density, it is observed that the values at the time of survey T1 are higher in areas where cover crop growth is limited (LV) (Table 6). The other two vigor conditions show a 12 % reduction in SBD. Conversely, in HV vigor zones, a 7 % lower water content is recorded compared to MV and a 15 % lower compared to LV, with the latter showing a statistically different value from HV. With reference to WFPS, that is considered an indicator of soil water availability and saturation, the highest value was recorded in LV zones. In these areas, WFPS is observed to be >30 % higher than in the MV and HV vigor zones. During the summer season, there is a 7 % increase in SBD value in the soil. In T2, differences between the areas of vigor were observed, confirming the findings of T1. In this case, LV zones had values 11 % higher than HV and MV. In terms of water content, a significant 60 % decrease in the amount of soil water was observed between seasons T1 and T2.

Fig. 9 shows the trend of soil organic carbon content; this parameter is stable between the periods T1 and T2; indeed, no difference is observed in terms of time. Nevertheless, statistically significant differences were found between the vigor levels in each epoch. In T1 the HV zones are characterised by a greater content than the LV zones, while an intermediate behaviour was observed for the MV zones. In the case of the T2, no difference was observed between HV and MV, however, in this phase, statistically significant differences can be attributed only to the LV zone compared to the other two.

The results of soil nitrogen monitoring during the two observation periods are presented in Fig. 10. Regarding stage T1, no significant differences were observed among the vigor zones, with a mean soil nitrogen content equal to 1.33 (g kg^{-1}). This trend was also confirmed in T2, where no statistically significant differences were observed among the vineyard vigor levels. However, it is important to note that soil nitrogen content is subject to seasonal fluctuations, in this study an increase in nitrogen content from stage T1 to T2 can be observed. In HV there was a 12 % increase over the year, reaching a value of 1.47 (g kg^{-1}) during grape ripening (T2). The dynamics of soil nitrogen content in MV zones are noteworthy, indeed, although nitrogen content was initially low in phase T1, there was a 20 % increase during stage T2, with values reaching 1.51 (g kg^{-1}). In contrast, no significant variations in soil nitrogen content were observed in LV zones, with only a slight 4 % increase. The main differences between the vigor levels can be recognised for the T2 season; actually, the MV vineyard zones show a higher nitrogen content of the soil in those areas than in the other vigor levels.

Table 6
Bulk density, water content and water filled pore space (WFPS) of soil determined in winter seasons (T1) and after grape harvest (T2). Different letters indicate significant differences (p-value < 0.01) among the three vigor levels.

Soil parameter	Vigor level		
	HV	MV	LV
T1			
Bulk density (g cm^{-3})	1.08 ± 0.03 **b**	1.10 ± 0.03 **b**	1.24 ± 0.01 **a**
Soil water content (%)	28.29 ± 1.61 **b**	30.05 ± 1.20 **ab**	34.53 ± 0.97 **a**
WFPS	55.66 ± 4.60 **b**	63.19 ± 1.93 **b**	86.30 ± 2.35 **a**
T2			
Bulk density (g cm^{-3})	1.16 ± 0.04 **b**	1.18 ± 0.03 **b**	1.30 ± 0.02 **a**
Soil water content (%)	12.36 ± 1.43	12.89 ± 0.22	10.63 ± 0.65 **n.s**
WFPS	21.12 ± 3.08	22.65 ± 0.89	24.00 ± 1.83 **n.s**

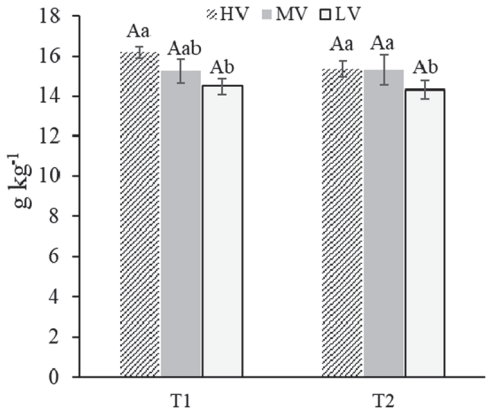

Fig. 9. Concentration of soil organic carbon (SOC) contents determined in T1 and T2 among the three vigor levels. Data were subjected to two-way ANOVA (Tukey's test, p-value < 0.01) capital letters indicate statistically significant difference among two periods, while the lowercase letters indicate differences among vigor levels. ± SE is shown with the bars.

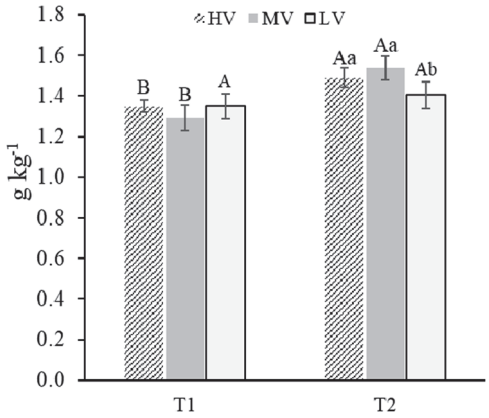

Fig. 10. Concentration of soil total nitrogen (TN) content determined in T1 and T2 among the three vigor levels. Data were subjected to two-way ANOVA (Tukey's test, p-value < 0.01) capital letters indicate statistically significant difference among two periods, while the lowercase letters indicate differences among vigor levels. ± SE is shown with the bars.

Principal Component Analysis (PCA) was carried out with the aim of reducing the number of linear combinations of variables that represent most of the data variability. In this study, PCA was performed for the two investigation periods, and it is displayed in table 7, treating the dataset of period T1 separately from the dataset of period T2. For the T2 dataset twelve components were extracted, collectively representing 100 % of the variability. In the case of the T1 dataset, the eigenvalues extracted from the correlation matrix show that the first two components of the PCA are sufficient to explain the total variance of the sample. In the analysis conducted for the T1 dataset, the first eigenvalue is (3.9850), and the second is (2.8712), while the other components have values below 1 and are not considered. The first principal component explains

Table 7
Principal component analysis of 8 variables for T1 and 12 for T2 dataset with eigenvalues and proportion of variability explained for the first five principal components (PC) with eigenvalues > 0.5.

	T1				
	PC 1	PC 2	PC 3	PC 4	PC 5
Eigenvalue	3.985	2.8712	0.8379	0.6645	0.5083
Proportion	0.498	0.359	0.075	0.031	0.037
	T2				
Eigenvalue	7.9391	2.3365	0.9804	0.8012	0.6567
Proportion	0.682	0.171	0.082	0.067	0.055

49.8 % of the total variance, and the second component explains 35.9 % of the total variance in the data. It can be stated that the first two components are sufficient to explain a significant portion of the variance of the entire dataset, as both collectively explain 85.7 %. In the case of the T2 dataset, based on the Kaiser criterion, the first two components can be considered. In fact, the first component of the PCA is characterized by an eigenvalue of (7.9391), and the second has an eigenvalue of (2.3365), while the other ten components have eigenvalues below 1 and are not considered to explain the model. On the other hand, the cumulative variation explained by the first two principal components is 0.85, meaning that the first two principal components explain over 85 % of the total variance in the data.

Eight factors were considered in the case of T1 dataset, corresponding to soil parameters (SBD, WFPS, SWC, N, SOC), cover crop biometric parameters (PL, CC-DW), and crop spectral response represented by NDVI. With the PCA performed for the T1 data set, eight components were extracted, collectively representing 100 % of the variability found in the original dataset. PCA was able to separate the different parameters by establishing precise patterns as observed in Fig. 11a. WFPS, SWC, N, SBD were positioned on the negative side of PCA. Instead, the soil parameter SOC, NDVI as well as the length of the cover crop (PL) and dry weight of cover crop biomass (CC-DW), opposed the previous group of parameters and were positioned in the positive quadrant of PC1. In Fig. 11b, the biplot of PCA referred to the T2 dataset is represented. In this case, the soil parameters such as SBD, WFPS, SWC, N, are placed in to the negative PC1 quadrant, except for the SOC parameter, which is in the opposite position, within the positive PC1 and PC2 quadrant. Regarding the vegetative parameters of the vineyard, represented by S.L, L.S, T.L.A, NBI, Chl, they are positioned in the quadrant of positive values of PC1 and negative of PC2. The parameter representing the spectral response of the vineyard (NDVI) is located near the vegetative parameters, and indeed it resides in the quadrant of positive values of PC1 and PC2. The vineyard yield parameter is set in an intermediate position relative to the clusters of soil parameters and that of the vegetative parameters of the vineyard; however, it leans towards the latter, and indeed it resides in the quadrants of positive values both of PC1 and PC2.

3.4. Soil penetration resistance

Table 8 presents the results of the analysis of variance (ANOVA), highlighting the significant effect of the three factors considered (Time, Depth, and Vigor) and their interactions on the observed response for the variable (SPR). Factor “time” shows a highly significant effect (P-Value <0.01), indicating significant differences between the two periods considered in the study. Similarly, the “depth” factor demonstrates a highly significant effect (P-Value <0.01), suggesting differences between SPR values at different soil depth levels. The statistical analysis revealed that both the "time" factor (F-value = 309.88) and the "depth" factor, (F-value = 233.25), significantly affect SPR. Specifically, "time" factor showed substantial differences among the means of the periods considered, while "depth" factor indicated notable variations among the means across different soil depth levels. The “vigor level” factor shows a highly significant effect (P-Value <0.01), indicating significant differences between vigor levels for both T1 and T2 periods. The interaction between time and vigor level is significant (P-Value = 0.002), indicating that the factors time and vigor are not independent, rather their interaction has a significant impact on the SPR variable. Similarly, the interaction between time and depth is significant (P-Value = 0.003), which means that at different soil depths, time may influence SPR to a different extent. However, the interaction between depth and vigor level is not significant (P-Value = 0.882). Finally, the residual error (0.1146) is relatively low, indicating that the model effectively explains the

Table 8
Within-subject ANOVA for soil penetration resistance (SPR) [MPa] (p-values < 0.01) as a function of the two investigation periods and the vigor levels considered.

Source of variation					
	DF	***Adj SS***	***Adj MS***	***F-Value***	***P-Value***
Time	1	3.5528	3.55279	309.88	<0.001
Depth	5	13.3712	2.67424	233.25	<0.001
Vigor level	2	1.219	0.60948	53.16	<0.001
Time*Depth	5	0.4553	0.09105	8.94	0.003
Time*Vigor level	2	0.2589	0.12943	19.29	0.002
Depth*Vigor level	10	0.0526	0.00526	0.46	0.882
Error	10	0.1146	0.01146		
Total	35	19.024			

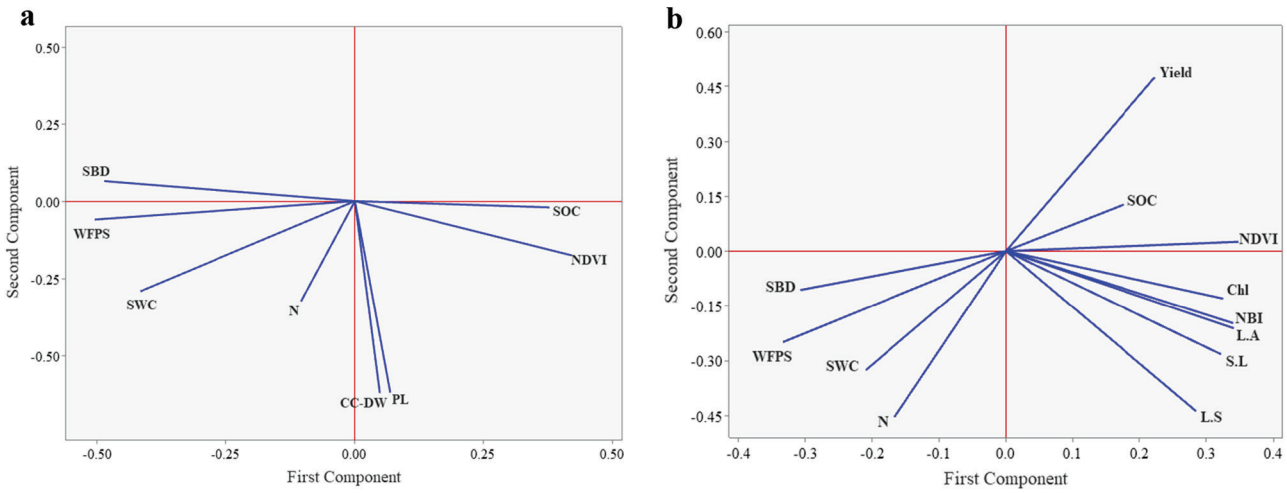

Fig. 11. Principal Components Analysis 2D plot of Component Weights.

observed variation for the data.

The average SPR values measured during T1, when the vineyard was managed with cover crop in the inter-row, and during T2, when the soil was bare, are shown in Fig. 12. SPR is represented in six depth intervals: 0 - 0.10 m, 0.11 - 0.20 m, 0.21–0.30 m, 0.31–0.40 m, 0.41–0.50 m, 0.51–0.60 m, respectively. No significant differences were observed in the depth 0 - 0.10 m between T1 and T2. Considering the depth 0.11-0.20 m, significant differences were observed, where SPR increased by 40 % between T1 and T2, going from 2.16 MPa in T1 to 3.05 MPa in T2. Soil penetration resistance values increased from T1 to T2 for all the considered depth layers.

The penetration resistance curves measured for T1 and T2 in the soil depth 0–0.60 m are illustrated in Fig. 13. Significant differences ($P < 0.01$) were found in SPR values among different vigor levels in each soil depth interval. Referring to T1, no significant differences were observed in SPR at a depth of 0–0.20 m, with LV (1.77 MPa) being the highest value in this layer. The highest SPR for the 0.21–0.30 m layer was found in LV (2.45 MPa), which is statistically different from MV and HV, which show values of 1.94 MPa and 2.08 MPa respectively. In the layer 0.31–0.40 m, the highest value is reported by LV (2.75 MPa), however it is worth mentioning that HV values (2.30 MPa) are statistically intermediate between LV and MV, the latter reporting the lowest value (2.12 MPa). For the levels below the depth of 0. 40 m, SPR is always greater in the LV zones, whereas no differences were found between HV and MV. Surveys performed during T2 sampling show that the LV zones are characterised by statistically higher SPR values than the other vigor levels. For example, high values of 2.21 and 3.39 MPa were recorded in the shallowest 0.10 m and 0.20 m layers, respectively. Comparing the LV values with those of MV, it is observed that the LV values are approximately 17 % higher than MV in the first soil layer (0–0.10 m). This difference is smaller in the second layer (0.21–0.30 m), where LV exceed MV by only 10 %. However, no statistically significant differences were found in this soil depth interval. Regarding the HV vigor zones, SPR values were always lower than LV and MV values. In the first soil layer, HV showed a value of 1.68 MPa about 30 % lower than LV. In the second depth layer (0.21–0.30 m), the SPR values measured for HV zones were about 25 % lower than LV zones. These results show a general upward trend in SPR for LV, which shows the highest values, followed by MV and HV. Furthermore, the SPR values follow the trends reported for the three vigor levels even for the underlying layers, at least up to a depth of 0.40 m statistically significant differences were observed. In these layers, HV showed the lowest SPR, with values of 2.94 MPa and 3.19 MPa respectively for the layers up to a depth of 0.50 m. In contrast, the measurements carried out in the LV zones are significantly higher, showing 3.50 MPa and 3.75 MPa respectively.

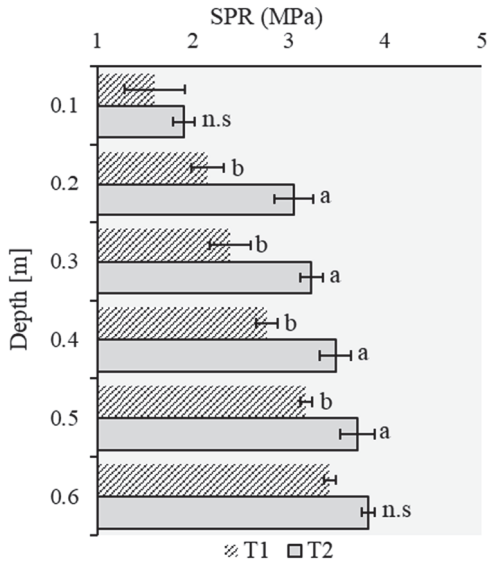

Fig. 12. Representation of soil penetration resistance for monitoring stages T1 and T2 divided by soil depth layers. Different letters indicate statistically significant differences between T1 and T2 for all depths (p-value < 0.01) based on Tukey's test.

4. Discussion

4.1. Evaluation of vegetation indices and variability

The aim of this study was to multi-temporally compare cover crop conditions during the winter season, when the vineyard was dormant, and the summer season, using both classical statistical methods and geospatial analysis. The study was carried out using information acquired from a UAV platform, subsequently, the degree of similarity of T1 and T2 datasets was assessed. The different behavior of HV and LV zones observed through NDVI remained consistent and was obtained both during the winter and the summer season. Regarding NDVI data, it is observed that the range of values reported for the three cover crop vigor levels is much wider than that observed for vine canopy. The wider range of values observed in Table 3 is particularly evident in the first measurement (T1). It can be attributed to the low NDVI values observed in LV zones of the cover crop, indicating low vegetation cover. In contrast, NDVI data in the HV zones are significantly higher, reflecting denser vegetation. This dissimilarity between NDVI values at different vigor levels contributes to the wider range of values. The low values observed during the winter season can be explained by considering first the high soil moisture conditions. Under moist soil conditions, water can significantly influence NIR reflectance (Merzlyak et al., 2002). Furthermore, these low values observed for the cover crop are mainly attributable to the LV zones, where cover crop growth was sparse. Bare soil has a high reflectance in the NIR, which can lead to a significant reduction in NDVI (Jensen, 2009). These findings are consistent with those identified by Yuan et al. (2019), where a significant spatial variability for cover crop NDVI was observed, with the average value ranging from 0.34 to 0.61 during the growth season. The NDVI observed for the vineyard, on the other hand, display a more limited range of variation among the three vigor levels. However, it was still possible to discriminate between the three vigor levels across the entire experimental plot. With reference to maps T2A and T2B, the NDVI for LV zones exceed the threshold of 0.5. This result is consistent with observations made by other authors, where by segmenting only pixels of trellised vine canopy, similar NDVI values were obtained (Caruso et al., 2023; Romboli et al., 2017). A relatively consistent spatial variability between vineyard and cover crop was observed. Thanks to the spatial autocorrelation maps derived from BILISA, it was possible to conduct a quantitative analysis of spatial variability between T1 and T2, providing a clear understanding of the multitemporal correspondence. Unlike visual analysis, this approach resolves issues associated with qualitative analysis (Matese et al., 2019). In reference to the cover crop and vineyard vigor maps, the highest correlation was found for the T1 dataset with T2B (MI = 0.54, Fig. 7). The spatial analysis conducted by BILISA revealed a significant presence of spatial dependence between the two georeferenced variables and some local differences in spatial heterogeneity. It is worth noting that inputs and cultural practices were uniformly applied across the entire plot. Cover crop cultivation in the inter-row was carried out on a temporary basis, exclusively during the winter season, for 8 consecutive years. Consequently, variations in vineyard and cover crop growth are primarily attributable to environmental factors, specifically soil chemical and physical conditions, as confirmed by several studies (Kotsaki et al., 2020; Tardáguila et al., 2011). Remote sensing of cover crops appears to be a viable option for assessing spatial variability of soil nutrient status. Leveraging the concept that cover crops serve as indicators of soil physical and chemical conditions, a study, conducted on an annual cash crop rather than a perennial crop, suggests that information on spatial variability can be

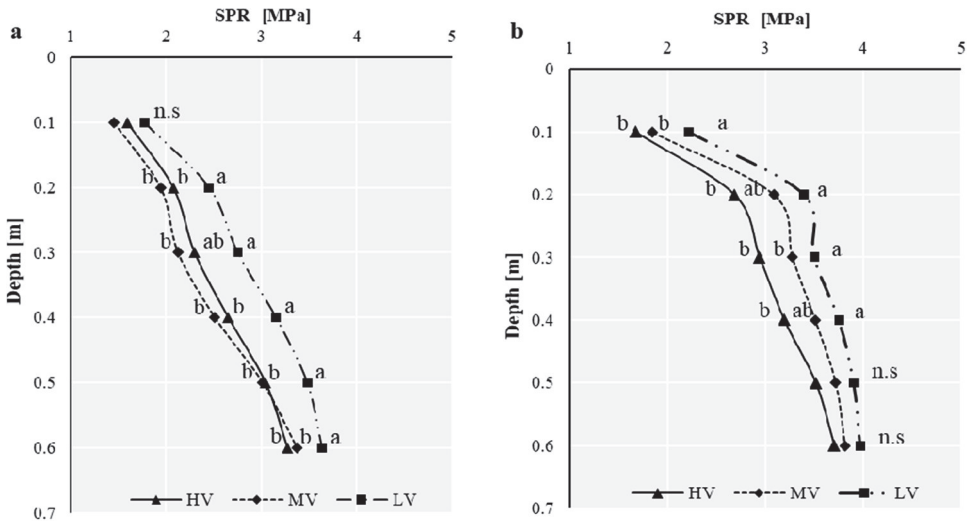

Fig. 13. Soil penetration resistance (SPR) in three vigor levels. **a**) T1; **b**) T2. Different letters indicate statistically significant differences among LV, MV and HV vigor levels for all soil depths (p-value < 0.01) based on Tukey's test.

utilized to enhance the management of cash crops (Futerman et al., 2023). Damian et al. (2017) conducted UAV monitoring on a cover crop followed by a cash crop, observing a positive correlation between the vigor maps of the two periods. Additionally, they noted that dry matter and accumulated soil nitrogen levels, assessed after cover crop termination, exhibited a positive correlation with cash crop yield variability.

4.2. *Effects of soil variability on crop's growth*

Subsequently, we delved deeper into the analysis to identify the reasons behind the observed variation in soil vigor levels. This allowed for a more thorough examination of the factors that could influence such variability. Overall, the soil physical properties, i.e. SWC, SBD and SPR observed through the measurements conducted for LV, MV and HV vigor zones on the two survey dates, showed significant differences. In this study, a clear temporal variation in SWC was observed. The temporal variation dynamics were characterized by a marked decrease in water content during the summer season, which influences other soil parameters (Vereecken et al., 2014). This could justify the increase in SBD value between T1 and T2. During the T2 stage, the decrease in SWC leads to soil compaction, as the previously water-filled voids are depleted. SPR can result in an increase in SBD, as soil particles tend to become closer to each other, thus increasing soil density (Shah et al., 2017). SWC is the most important factor influencing soil compaction processes (Soane and van Ouwerkerk, 2013). When soil loses water, its cohesion and consistency properties may decrease, making it more susceptible to compaction and structural loss, thereby contributing to an increase in SPR (Håkansson and Lipiec, 2000; Lipiec et al., 2002). Regarding period T1, the differences observed in the vigor levels are mainly related to the soil's physical properties. During T1, the highest SWC percentage was observed in LV mainly due to lower water infiltration along the soil profile. This phenomenon is primarily due to reduced water infiltration along the soil profile (Hamza and Anderson, 2005), there is excess soil moisture that can be attributed to increased SPR, as evidenced by the high SBD observed for LV areas, during the T1 phase. Soil compaction reduces total porosity, resulting in decreased soil hydraulic conductivity (Pagliai et al., 2003), thus, WFPS parameter in LV zones was statistically higher. This phenomenon is also supported by the data in Table 4, in which during T1, cover crop in LV zones exhibited shorter plant length, lower fresh weight, lower dry weight biomass, leading to a reduced NDVI (Table 3). Reduced water infiltration may reduce oxygen supply to the roots, triggering a shift in their metabolism, including increased anaerobic respiration and greater utilization of reserve carbohydrates, ultimately reducing overall development (Jackson and Colmer, 2005). However, the differences in SPR values observed among the vigor levels are primarily attributable to the higher presence of organic matter, as observed in HV and MV zones. Scientific literature has demonstrated that an increase in SOC content results in greater total porosity, contributing to lower SBD and consequently reducing penetration resistance (Celik et al., 2010; Haruna et al., 2020). The variability observed in SOC content among the vigor levels (Fig. 13) influenced SPR, which exhibited higher values in LV zones where SOC content was low. Comparison of SPR curves for the three vigor levels revealed that this parameter increased with soil depth, likely due to overload pressure generated by agricultural machinery traffic (Carrara et al., 2007). For both period T1 and T2, in layers below 0.2 m, the SPR value tends to increase, exceeding the critical threshold for root development (Whalley et al., 2007). This phenomenon is more pronounced in LV zones compared to MV and HV zones. This occurrence may have led to such differences in root development between the vigor areas, indeed, the root system of *Vicia faba*, like other legumes, tends to develop deep following the soil profile (Kocira et al., 2020). SPR values during the summer period (T2) are high when compared to the critical threshold for vine root elongation. Other studies conducted in Mediterranean environments report comparable values to those observed in this vineyard (Catania et al., 2013; López-Piñeiro et al., 2013). Nevertheless, the observed differences between MV vigor compared to LV zones during T2 stage are attributed to a higher bulk density. Pereyra et al. (2023) found that grapevines in LV zones were characterized by 70 % of roots thinner than 2 mm positioned in the top 0.30 m deep layer of soil, and no roots were observed below 0.5 m. Consistent with previous experiments, it can be supposed that the increased growth of cover crops observed during the winter season (T1) for MV and HV released more residues into the soil, which led to reduced soil compaction (Muñoz et al., 2007). In these zones, the increased growth of cover crops may also explain the higher accumulation of total N in the soil (Fig. 10). The increase in total N from period T1 to period T2 was significant. This result is justified by the rapid mineralization process of N to which residues of leguminous cover crops are subjected; moreover, through rhizodeposition, roots manage to fix satisfactory amounts of nitrogen (Kocira et al., 2020). Therefore, the higher presence of easily assimilable N in the soil and lower values of SBD and SPR contributed to improving the vine nitrogen status observed in HV and MV. This result is in line with what was observed by Pereyra et al. (2023), where a higher concentration of N in soil was measured for HV zones, furthermore, these vines were characterized by a higher leaf N content. Similarly, this study observed that

LV zones had a lower leaf N content compared to HV and MV (Fig. 6b). These results confirm that vine leaf N content is an diagnostic tool for identifying vigor levels (Balachandra et al., 2009; Gatti et al., 2022).

Soil physical-chemical variability has shown a significant influence on crop growth and spectral response through NDVI obtained from UAVs. The results of this study are consistent with those reported by Yeom et al. (2019), who examined crop spectral response in relation to different soil management conditions. In particular, the authors show that an increase in SBD and SPR results in changes in crop spectral response. Both for cover crops and for vineyard in HV and MV zones, low reflectance is recorded for the red band, due to high chlorophyll activity, while the NIR band is strongly reflected (Haboudane et al., 2008). This phenomenon could indirectly explain the high chlorophyll content measured for the leaves of HV and MV vines (Fig. 6a), consequently inducing an increase in NDVI. However, a study conducted by (Martins et al., 2021) used UAVs equipped with multispectral cameras to analyze herbaceous crops cultivated with different soil management practices and found no significant differences in the spectral response. The authors attribute the lack of differences to the relatively low SBD and SPR values, which did not reach thresholds that would affect root development.

5. Conclusions

The current study found new information regarding soil and vineyard agroecosystem interactions. The study of soil variability parameters uncovered interesting information on the influence of the spectral response of the vineyard and cover crop. Using remote sensing, clusters of plants with the highest vegetative growth capacity were identified. In comparison, significant differences in vegetative growth between the two crops were observed in the same areas. The main differences can be attributed to reduced SOC content and consequently higher SBD and SPR. In addition, SPR for LV vigor remained significantly higher ($p < 0.01$) for all the depths and for both periods. Both crops show similar behavior under the same soil conditions. In addition, it can be stated that the reduction of cover crop growth influence soil properties. Conversely, in areas where cover crop produces more biomass, it contributes to maintaining or improving the overall soil condition, with a net benefit to the vineyard. Cover crops variability has an influence on vine growth, with this in mind using the information derived from remote sensing of cover crops can enable better planning of precision vineyard management.

Disclosure

After using this tool/service, the author(s) reviewed and edited the content as needed and take(s) full responsibility for the content of the publication, in alignment with the ICMJE, (2023) codex.

CRediT authorship contribution statement

Pietro Catania: Writing – review & editing, Supervision, Project administration, Methodology, Investigation, Funding acquisition, Conceptualization. **Massimo Vincenzo Ferro:** Writing – original draft, Visualization, Software, Data curation. **Santo Orlando:** Validation, Supervision, Software, Methodology, Data curation. **Mariangela Vallone:** Writing – review & editing, Writing – original draft, Supervision, Software, Investigation, Formal analysis.

Declaration of competing interest

The authors of this article declare that they have no conflicts of interest that could influence the objectivity of the research or the presentation of the results.

The authors have no financial or other relationships that could negatively affect the objectivity of the research or its presentation. This scientific paper was prepared entirely independently and was not influenced by third parties or personal interests. The authors ensure that the research presented in this paper was conducted in an ethical and transparent manner in accordance with the editorial guidelines of the journal *Scientia Horticulturae*.

Acknowledgments

This work was supported by the Ministero dell'Agricoltura, della sovranità alimentare e delle foreste, Italy. [Bando Vitivinicolo 2023, Project title: Applicazione della viticoltura di precisione per l'ottimizzazione del processo produttivo in ambiente mediterraneo. CUP: B73C23001330001].

Data availability

Data will be made available on request.

References

Anselin, L., & Rey, S.J. (2014). Modern spatial econometrics in practice: a guide to GeoDa, GeoDaSpace and PySAL. (No Title).

ASAE. (2009). *Procedures for Using and Reporting Data Obtained with the Soil Cone Penetrometer. Test.*.

Balachandra, L., Edis, R., White, R., Chen, D., 2009. The relationship between grapevine vigour and N-mineralization of soil from selected cool climate vineyards in Victoria, Australia. J. Wine Res. 20 (3), 183–198.

Basso, B., Ritchie, J., Pierce, F., Braga, R., Jones, J., 2001. Spatial validation of crop models for precision agriculture. Agric. Syst. 68 (2), 97–112.

Bhandral, R., Saggar, S., Bolan, N., Hedley, M., 2007. Transformation of nitrogen and nitrous oxide emission from grassland soils as affected by compaction. Soil Tillage Res. 94 (2), 482–492.

Blake, G., Hartge, K., 1986. Particle density. Methods of Soil Analysis: Part 1 Physical and Mineralogical Methods 5, 377–382.

Bollas, N., Kokinou, E., Polychronos, V., 2021. Comparison of sentinel-2 and UAV multispectral data for use in precision agriculture: an application from northern greece. Drones 5 (2), 35.

Campos, J., García-Ruíz, F., Gil, E., 2021. Assessment of vineyard canopy characteristics from vigour maps obtained using UAV and satellite imagery. Sensors 21 (7), 2363.

Carrara, M., Castrignanò, A., Comparetti, A., Febo, P., Orlando, S., 2007. Mapping of penetrometer resistance in relation to tractor traffic using multivariate geostatistics. Geoderma 142 (3–4), 294–307.

Caruso, G., Palai, G., Tozzini, L., D'Onofrio, C., Gucci, R., 2023. The role of LAI and leaf chlorophyll on NDVI estimated by UAV in grapevine canopies. Sci. Hortic. 322, 112398.

Caruso, G., Tozzini, L., Rallo, G., Primicerio, J., Moriondo, M., Palai, G., Gucci, R., 2017. Estimating biophysical and geometrical parameters of grapevine canopies ('Sangiovese') by an unmanned aerial vehicle (UAV) and VIS-NIR cameras. Vitis 56 (2), 63–70.

Catania, P., Badalucco, L., Laudicina, V.A., Vallone, M., 2018. Effects of tilling methods on soil penetration resistance, organic carbon and water stable aggregates in a vineyard of semiarid Mediterranean environment. Environ Earth Sci 77, 1–9.

Catania, P., Vallone, M., Pipitone, F., Argento, G.F., Spartà, G., Laudicina, V.A., 2013. Soil management effect on soil penetration resistance in the vineyard. J. Agric. Eng. 44 (s2).

Celik, I., Gunal, H., Budak, M., Akpinar, C., 2010. Effects of long-term organic and mineral fertilizers on bulk density and penetration resistance in semi-arid Mediterranean soil conditions. Geoderma 160 (2), 236–243.

Chiles, J.-P., Delfiner, P., 2009. Geostatistics: Modeling spatial Uncertainty. John Wiley & Sons. Vol. 497.

Czyż, E.A., 2004. Effects of traffic on soil aeration, bulk density and growth of spring barley. Soil Tillage Res. 79 (2), 153–166.

Damian, J.M., Santi, A.L., Fornari, M., Da Ros, C.O., Eschner, V.L., 2017. Monitoring variability in cash-crop yield caused by previous cultivation of a cover crop under a no-tillage system. Comput. Electron. Agric. 142, 607–621.

Dexter, A., 2004. Soil physical quality: part I. Theory, effects of soil texture, density, and organic matter, and effects on root growth. Geoderma 120 (3–4), 201–214.

FAO, I., 2006. ISRIC: world reference base for soil resource in world soil resource report no. 103. FAO. *Rome, Italy*.

Ferro, M.V., Catania, P., 2023. Technologies and innovative methods for precision viticulture: a comprehensive review. Horticulturae 9 (3), 399.

Ferro, M.V., Catania, P., Miccichè, D., Pisciotta, A., Vallone, M., Orlando, S., 2023. Assessment of vineyard vigour and yield spatio-temporal variability based on UAV high resolution multispectral images. Biosystems Eng. 231, 36–56. https://doi.org/10.1016/j.biosystemseng.2023.06.001.

Filippetti, I., Allegro, G., Valentini, G., Pastore, C., Colucci, E., Intrieri, C., 2013. Influence of vigour on vine performance and berry composition of cv. Sangiovese (Vitis vinifera L.). OENO One 47 (1), 21–33.

Fillery, I., 2001. The fate of biologically fixed nitrogen in legume-based dryland farming systems: a review. Aust. J. Exp. Agric. 41 (3), 361–381.

Futerman, S.I., Laor, Y., Eshel, G., Cohen, Y., 2023. The potential of remote sensing of cover crops to benefit sustainable and precision fertilization. Sci. Total Environ. 891, 164630.
Gatti, M., Garavani, A., Squeri, C., Diti, I., De Monte, A., Scotti, C., Poni, S., 2022. Effects of intra-vineyard variability and soil heterogeneity on vine performance, dry matter and nutrient partitioning. Precision Agriculture 23, 150–177.
Guerra, B., Steenwerth, K., 2012. Influence of floor management technique on grapevine growth, disease pressure, and juice and wine composition: a review. Am. J. Enol. Vitic. 63 (2), 149–164.
Guzmán, G., Cabezas, J.M., Sánchez-Cuesta, R., Lora, Á., Bauer, T., Strauss, P., Winter, S., Zaller, J., Gómez, J., 2019. A field evaluation of the impact of temporary cover crops on soil properties and vegetation communities in southern Spain vineyards. Agric. Ecosyst. Environ. 272, 135–145.
Haboudane, D., Tremblay, N., Miller, J.R., Vigneault, P., 2008. Remote estimation of crop chlorophyll content using spectral indices derived from hyperspectral data. IEEE Trans. Geosci. Remote Sens. 46 (2), 423–437.
Håkansson, I., Lipiec, J., 2000. A review of the usefulness of relative bulk density values in studies of soil structure and compaction. Soil Tillage Res. 53 (2), 71–85.
Hamza, M., Anderson, W.K., 2005. Soil compaction in cropping systems: a review of the nature, causes and possible solutions. Soil Tillage Res. 82 (2), 121–145.
Haruna, S.I., Anderson, S.H., Udawatta, R.P., Gantzer, C.J., Phillips, N.C., Cui, S., Gao, Y., 2020. Improving soil physical properties through the use of cover crops: a review. Agrosystems, Geosci. Environ. 3 (1), e20105.
Hati, K.M., Swarup, A., Dwivedi, A., Misra, A., Bandyopadhyay, K., 2007. Changes in soil physical properties and organic carbon status at the topsoil horizon of a vertisol of central India after 28 years of continuous cropping, fertilization and manuring. Agric. Ecosyst. Environ. 119 (1–2), 127–134.
Haynes, R.J., Naidu, R., 1998. Influence of lime, fertilizer and manure applications on soil organic matter content and soil physical conditions: a review. Nutr. Cycling Agroecosyst. 51, 123–137.
Hirschmuller, H., 2005. Accurate and efficient stereo processing by semi-global matching and mutual information 2, 807–814.
Jackson, M., Colmer, T., 2005. Response and adaptation by plants to flooding stress. Ann. Bot. 96 (4), 501–505.
Jensen, J.R., 2009. Remote Sensing of the environment: An earth Resource Perspective 2/e. Pearson Education India.
Karn, R., Hillin, D., Helwi, P., Scheiner, J., Guo, W., 2024. Assessing grapevine vigor as affected by soil physicochemical properties and topographic attributes for precision vineyard management. Sci. Hortic. 328, 112857.
Kaye, J.P., Quemada, M., 2017. Using cover crops to mitigate and adapt to climate change. A review. Agron. Sustainable Dev. 37, 1–17.
Kocira, A., Staniak, M., Tomaszewska, M., Kornas, R., Cymerman, J., Panasiewicz, K., Lipińska, H., 2020. Legume cover crops as one of the elements of strategic weed management and soil quality improvement. A review. Agriculture 10 (9), 394.
Kotsaki, E., Reynolds, A.G., Brown, R., Lee, H.-S., Jollineau, M., 2020. Spatial variability in soil and vine water status in Ontario vineyards: relationships to yield and berry composition. Am. J. Enol. Vitic. 71 (2), 132–148.
Kottek, M., Grieser, J., Beck, C., Rudolf, B., & Rubel, F. (2006). *World map of the Köppen-Geiger climate classification updated*.
Laudicina, V., Barbera, V., Gristina, L., Badalucco, L., 2012. Management practices to preserve soil organic matter in semiarid Mediterranean environment. Soil Organic matter: Ecology, Environmental Impact and Management. Nova Science Publishers, Inc, pp. 39–61.
Legendre, P., Fortin, M.J., 1989. Spatial Pattern and Ecological Analysis, 80. Vegetatio, pp. 107–138.
Lipiec, J., Ferrero, A., Giovanetti, V., Nosalewicz, A., Turski, M., 2002. Response of structure to simulated trampling of woodland soil. Adv. Geoecol 35, 133–140.
López-Piñeiro, A., Muñoz, A., Zamora, E., Ramírez, M., 2013. Influence of the management regime and phenological state of the vines on the physicochemical properties and the seasonal fluctuations of the microorganisms in a vineyard soil under semi-arid conditions. Soil Tillage Res. 126, 119–126.
Martins, R.N., Portes, M.F., e Moraes, H.M.F., Junior, M.R.F., Rosas, J.T.F., Junior, W.de A.O., 2021. Influence of tillage systems on soil physical properties, spectral response and yield of the bean crop. Remote Sens. Appl.: Society and Environ. 22, 100517.
Matese, A., Di Gennaro, S.F., 2021. Beyond the traditional NDVI index as a key factor to mainstream the use of UAV in precision viticulture. Sci. Rep. 11 (1), 1–13.
Matese, A., Di Gennaro, S.F., Santesteban, L.G., 2019. Methods to compare the spatial variability of UAV-based spectral and geometric information with ground autocorrelated data. A case of study for precision viticulture. Comput. Electron. Agric. 162, 931–940.
McArtney, S., Ferree, D., 1999. Root and cane pruning affect vegetative development, fruiting, and dry-matter accumulation of grapevines. HortScience 34 (4), 617–621.
Merzlyak, M.N., Chivkunova, O.B., Melø, T., Naqvi, K.R., 2002. Does a leaf absorb radiation in the near infrared (780–900 nm) region? A new approach to quantifying optical reflection, absorption and transmission of leaves. Photosyn. Res. 72, 263–270.
Michel, J., Youssefi, D., Grizonnet, M., 2014. Stable mean-shift algorithm and its application to the segmentation of arbitrarily large remote sensing images. IEEE Trans. Geosci. Remote Sens. 53 (2), 952–964.
Moran, P.A., 1948. The interpretation of statistical maps. Journal of the Royal Statistical Society. Series B (Methodological) 10 (2), 243–251.
Muñoz, A., López-Piñeiro, A., Ramírez, M., 2007. Soil quality attributes of conservation management regimes in a semi-arid region of south western Spain. Soil Tillage Res. 95 (1–2), 255–265.
Nelson, D.a, Sommers, L., 1983. Total carbon, organic carbon, and organic matter. Methods of Soil Analysis: Part 2 Chem. Microbiolog. Properties 9, 539–579.
Novara, A., Gristina, L., Saladino, S., Santoro, A., Cerdà, A., 2011. Soil erosion assessment on tillage and alternative soil managements in a Sicilian vineyard. Soil Tillage Res. 117, 140–147.
Novara, A., Minacapilli, M., Santoro, A., Rodrigo-Comino, J., Carrubba, A., Sarno, M., Venezia, G., Gristina, L., 2019. Real cover crops contribution to soil organic carbon sequestration in sloping vineyard. Sci. Total Environ. 652, 300–306.
Novara, A., Pisciotta, A., Minacapilli, M., Maltese, A., Capodici, F., Cerdà, A., Gristina, L., 2018. The impact of soil erosion on soil fertility and vine vigor. A multidisciplinary approach based on field, laboratory and remote sensing approaches. Sci. Total Environ. 622, 474–480.
Ovalle, C., Del Pozo, A., Peoples, M.B., Lavín, A., 2010. Estimating the contribution of nitrogen from legume cover crops to the nitrogen nutrition of grapevines using a 15 N dilution technique. Plant Soil 334, 247–259.
Ozpinar, S., Ozpinar, A., Cay, A., 2018. Soil management effect on soil properties in traditional and mechanized vineyards under a semiarid Mediterranean environment. Soil Tillage Res. 178, 198–208.
Pádua, L., Marques, P., Adão, T., Guimarães, N., Sousa, A., Peres, E., Sousa, J.J., 2019. Vineyard variability analysis through UAV-based vigour maps to assess climate change impacts. Agronomy 9 (10), 581.
Pagliai, M., Marsili, A., Servadio, P., Vignozzi, N., Pellegrini, S., 2003. Changes in some physical properties of a clay soil in Central Italy following the passage of rubber tracked and wheeled tractors of medium power. Soil Tillage Res. 73 (1–2), 119–129.
Pastonchi, L., Di Gennaro, S.F., Toscano, P., Matese, A., 2020. Comparison between satellite and ground data with UAV-based information to analyse vineyard spatio-temporal variability: this article is published in cooperation with the XIIIth International Terroir Congress November 17-18 2020, Adelaide, Australia. Guest editors: cassandra Collins and Roberta De Bei. Oeno One 54 (4), 919–934.
Peel, M.C., Finlayson, B.L., McMahon, T.A., 2007. Updated world map of the Köppen-Geiger climate classification. Hydrol. Earth Syst. Sci. 11 (5), 1633–1644.
Pereyra, G., Pellegrino, A., Ferrer, M., Gaudin, R., 2023. How soil and climate variability within a vineyard can affect the heterogeneity of grapevine vigour and production. OENO One 57 (3), 297–313.
Puig-Montserrat, X., Stefanescu, C., Torre, I., Palet, J., Fabregas, E., Dantart, J., Arrizabalaga, A., Flaquer, C., 2017. Effects of organic and conventional crop management on vineyard biodiversity. Agric. Ecosyst. Environ. 243, 19–26.
R Core Team, 2023. R: a Language and Environment for Statistical Computing. Available. R Foundation for Statistical Computing, Vienna, Austria. https://www.R-project.org/.
Rey, S.J., Anselin, L., 2009. PySAL: a Python library of spatial analytical methods. Handbook of Applied Spatial analysis: Software tools, Methods and Applications. Springer, pp. 175–193.
Romboli, Y., Di Gennaro, S., Mangani, S., Buscioni, G., Matese, A., Genesio, L., Vincenzini, M., 2017. Vine vigour modulates bunch microclimate and affects the composition of grape and wine flavonoids: an unmanned aerial vehicle approach in a Sangiovese vineyard in Tuscany. Aust. J. Grape Wine Res. 23 (3), 368–377.
Rouse, J.W., Haas, R.H., Schell, J.A., Deering, D.W., & Harlan, J.C. (1974). Monitoring the vernal advancement and retrogradation (green wave effect) of natural vegetation. *NASA/GSFC Type III Final Report, Greenbelt, Md*, 371.
Shah, A.N., Tanveer, M., Shahzad, B., Yang, G., Fahad, S., Ali, S., Bukhari, M.A., Tung, S. A., Hafeez, A., Souliyanonh, B., 2017. Soil compaction effects on soil health and cropproductivity: an overview. Environ. Sci. Pollut. Res. 24, 10056–10067.
Shennan, C., 1992. Cover crops, nitrogen cycling, and soil properties in semi-irrigated vegetable production systems. HortScience 27 (7), 749–754.
Soane, B.D., van Ouwerkerk, C., 2013. Soil Compaction in Crop Production. Elsevier.
Sozzi, M., Kayad, A., Marinello, F., Taylor, J., Tisseyre, B., 2020. Comparing vineyard imagery acquired from Sentinel-2 and Unmanned Aerial Vehicle (UAV) platform. Oeno One 54 (2), 189–197.
Sumner, M.E., Miller, W.P., 1996. Cation exchange capacity and exchange coefficients. Methods of Soil Analysis: Part 3 Chem. Methods 5, 1201–1229.
Tardáguila, J., Baluja, J., Arpon, L., Balda, P., Oliveira, M., 2011. Variations of soil properties affect the vegetative growth and yield components of “Tempranillo” grapevines. Precision Agriculture 12 (5), 762–773.
Tremblay, N., Wang, Z., Cerovic, Z.G., 2012. Sensing crop nitrogen status with fluorescence indicators. A review. Agron. Sustainable Dev. 32, 451–464.
Vereecken, H., Huisman, J., Pachepsky, Y., Montzka, C., Van Der Kruk, J., Bogena, H., Weihermüller, L., Herbst, M., Martinez, G., Vanderborght, J., 2014. On the spatio-temporal dynamics of soil moisture at the field scale. J. Hydrol. 516, 76–96.
Webster, R., Oliver, M.A., 2007. Geostatistics For Environmental Scientists. John Wiley & Sons.
Whalley, W., To, J., Kay, B., Whitmore, A., 2007. Prediction of the penetrometer resistance of soils with models with few parameters. Geoderma 137 (3–4), 370–377.
Wheaton, A., McKenzie, B., Tisdall, J.M., 2008. Management to increase the depth of soft soil improves soil conditions and grapevine performance in an irrigated vineyard. Soil Tillage Res. 98 (1), 68–80.
Wichern, F., Eberhardt, E., Mayer, J., Joergensen, R.G., Müller, T., 2008. Nitrogen rhizodeposition in agricultural crops: methods, estimates and future prospects. Soil Biol. Biochem. 40 (1), 30–48.
Yeom, J., Jung, J., Chang, A., Ashapure, A., Maeda, M., Maeda, A., Landivar, J., 2019. Comparison of vegetation indices derived from UAV data for differentiation of tillage effects in agriculture. Remote Sens (Basel) 11 (13), 1548.
Yuan, M., Burjel, J., Isermann, J., Goeser, N., Pittelkow, C., 2019. Unmanned aerial vehicle–based assessment of cover crop biomass and nitrogen uptake variability. J. Soil Water Conserv. 74 (4), 350–359.